NASA TECHNICAL NOTE

NASA TN D-4869

NASA TN D-4869

REAL-HELIUM HYPERSONIC FLOW PARAMETERS FOR PRESSURES TO 3600 ATMOSPHERES AND TEMPERATURES TO 15 000° K

by Charles G. Miller III and Sue E. Wilder

Langley Research Center
Langley Station, Hampton, Va.

NATIONAL AERONAUTICS AND SPACE ADMINISTRATION • WASHINGTON, D. C. • NOVEMBER 1968

NASA TN D-4869

REAL-HELIUM HYPERSONIC FLOW PARAMETERS FOR PRESSURES TO 3600 ATMOSPHERES AND TEMPERATURES TO 15 000° K

By Charles G. Miller III and Sue E. Wilder

Langley Research Center
Langley Station, Hampton, Va.

NATIONAL AERONAUTICS AND SPACE ADMINISTRATION

For sale by the Clearinghouse for Federal Scientific and Technical Information
Springfield, Virginia 22151 – CFSTI price $3.00

REAL-HELIUM HYPERSONIC FLOW PARAMETERS FOR PRESSURES TO 3600 ATMOSPHERES AND TEMPERATURES TO 15 000° K

By Charles G. Miller III and Sue E. Wilder
Langley Research Center

SUMMARY

The virial form of the equation of state is used to derive a method for determining reservoir, nozzle-throat, free-stream, and normal-shock conditions for real-helium flow. This method is derived primarily to meet the needs of hotshot-type wind tunnels where the basic input data are measured reservoir pressure and stagnation pressure behind a normal shock. However, the method is derived to include an additional measurement of free-stream density, free-stream velocity, or reservoir temperature. The method is applied for reservoir pressures to 3600 atmospheres, temperatures to 15 000° K, and a range of free-stream Mach numbers from 10 to 100, and the results are presented in the form of nondimensionalized reservoir thermodynamic and nozzle-throat parameters and as simple correction factors which may be applied to ideal-helium flow parameters. These calculations are restricted to reservoir densities less than the critical density of helium and to theoretically uncondensed free-stream flow.

INTRODUCTION

Recent tests in the Langley hotshot tunnel have demonstrated the feasibility of operating this facility with helium as the test gas at Mach numbers from approximately 30 to 80. These preliminary results were obtained for reservoir pressures from approximately 200 to 1000 atmospheres and reservoir temperatures from 800° to 4000° K. For these reservoir conditions, appreciable errors can result from neglecting real-gas effects in determining the flow parameters (refs. 1 and 2). Therefore, a method employing the virial form of the equation of state was derived for determining reservoir, nozzle-throat, test-section free-stream, and test-section normal-shock conditions in real helium and is applicable for reservoir temperatures from 200° to 15 000° K.

This method was derived to be used primarily with measured reservoir and test-section stagnation pressures as inputs and was based on the assumption of uniform density throughout the reservoir during a tunnel test. In the event that another measurement such as free-stream density, free-stream velocity, or reservoir temperature is made to avoid

the assumption of uniform density throughout the reservoir, the method was also derived with the capability of utilizing an additional measurement as input.

Real-helium correction factors (ratio of real-helium value of a particular flow parameter to its ideal-helium value) were calculated and presented in the form of working charts for reservoir pressures to 3600 atmospheres, reservoir temperatures to 15 000° K, and a range of free-stream Mach numbers from 10 to 100. A similar technique was used in reference 1 for which approximate results were obtained above 590° K using the Beattie-Bridgeman equation of state with constants which were determined from experimental data obtained at temperatures up to only 590° K. The present method employing the virial equation of state, for which the virial coefficients of helium were obtained from references 3 to 7 for temperatures up to 15 000° K, was used to obtain more accurate real-helium effects for temperatures above 590° K. The present calculations are restricted to reservoir densities less than the critical density of helium and to theoretically uncondensed free-stream flow.

SYMBOLS

a	speed of sound
a_r	reference speed of sound
A	area
B	second virial coefficient
C	third virial coefficient
c_p	specific heat at constant pressure
c_v	specific heat at constant volume
d	diameter
D	fourth virial coefficient
h	specific enthalpy
M	Mach number

p	pressure
q	dynamic pressure
R	universal gas constant
s	specific entropy
T	temperature
U	velocity
V	reservoir volume
Z	compressibility factor
γ	ratio of specific heats
μ	coefficient of viscosity
ρ	density
ρ_{cr}	critical density
τ	time

Subscripts:

c	initial reservoir conditions
calc	calculated
con	condensed
i	ideal-gas conditions
m	measured

t,1 reservoir stagnation conditions

t,2 stagnation conditions behind normal shock

∞ free-stream conditions

2 static conditions immediately downstream of shock

Superscripts:

~ approximate value

* nozzle-throat conditions

BASIC THERMODYNAMIC RELATIONS

The virial form of the equation of state is used in conjunction with various thermodynamic relations to determine expressions for enthalpy, entropy, speed of sound, and specific heats, each as a function of density and temperature.

The virial form of the equation of state of a pure gas can be written as

$$p = \rho RT\left[1 + \rho B(T) + \rho^2 C(T) + \rho^3 D(T) + \ldots\right] = \rho RTZ \tag{1}$$

where $B(T)$, $C(T)$, $D(T)$, . . ., are the virial coefficients and are functions only of the temperature. The second virial coefficient $B(T)$ represents the deviations from the ideal-gas state arising from interactions involving two molecules of the gas; the third virial coefficient $C(T)$ represents deviation arising from interactions involving three molecules; and so forth. In the present study, interactions involving five or more atoms are neglected; hence, the compressibility factor Z was determined from

$$Z = 1 + \rho B(T) + \rho^2 C(T) + \rho^3 D(T) \tag{2}$$

The second, third, and fourth virial coefficients of helium were determined by Amdur and Mason (ref. 7) for a temperature range of 1000° to $15\,000^{\circ}$ K. The interatomic force laws used to determine the virial coefficients were derived from molecular-beam-scattering measurements. The virial coefficients of reference 7 for helium are

$$B(T) \approx (1.3436 \times 10^{-2})(15.8922 - \ln T)^3 + \ldots \tag{3}$$

$$C(T) \approx (9.0263 \times 10^{-5})(15.8922 - \ln T)^6 \tag{4}$$

and

$$D(T) \approx \left(7.0341 \times 10^{-7}\right)(15.8922 - \ln T)^9 \tag{5}$$

where B(T), C(T), and D(T) are in $cm^3/mole$, $(cm^3/mole)^2$, and $(cm^3/mole)^3$, respectively, for T in ^oK. The contribution to B(T) of the second and subsequent terms of equation (3) as presented in reference 7 is negligible and is therefore omitted. As shown in figure 1, where the second virial coefficient is plotted as a function of temperature, the values of B(T) obtained from equation (3) for temperatures less than about 1000^o K differ from the experimental results of references 3 to 6, with this discrepancy decreasing with increasing temperature. The second virial coefficient is negative at very low temperatures as a result of the atomic attraction forces, becomes positive at somewhat higher temperatures as repulsion forces start to dominate, passes through a maximum, and then decreases with further increase in temperature as the repulsion forces dominate. Therefore, this discrepancy between the calculated values of B(T) from equation (3) as obtained from reference 7, and the experimental results of references 3 to 6 is not unexpected since equation (3) is valid only in the temperature region where repulsion forces completely dominate. Also shown in figure 1 are values of B(T) obtained from the relation of reference 2

$$B(T) \approx \left(1.3436 \times 10^{-2}\right)(15.8922 - \ln T)^3 - 4.39 \exp\left[-\left(2.4177 \times 10^{-3}\right) T\right] \tag{6}$$

This relation is a modification of equation (3); the addition of a negative exponential term makes it agree more closely with the experimental results of references 3 to 6 for temperatures down to 300^o K. Following the example of reference 2, equation (3) was modified in a similar manner to yield the relation

$$B(T) \approx \left(1.3436 \times 10^{-2}\right)(15.8922 - \ln T)^3 - 8.04 \exp\left[-\left(3.7156 \times 10^{-3}\right) T\right] \tag{7}$$

Equation (7) extends the temperature range of equation (3) down to the region of maximum B(T), which occurs at about 200^o K (see fig. 1) and will be used herein. The exponential term of equation (7) is negligible for temperatures greater than about 2000^o K. The third and fourth virial coefficients agree reasonably well with experimental data for temperatures as low as 300^o K (ref. 7). According to reference 7, the error incurred in using equation (3), and hence in using equation (7), may be as high as 5 to 10 percent for the present temperature range whereas errors incurred in using equations (4) and (5) may be as high as 25 percent. However, the virial coefficients B(T), C(T), and D(T) represent perturbations in the ideal-gas behavior of helium to the first, second, and third order, respectively. Hence, as pointed out in reference 7, relatively large errors in the virial coefficients represent only small errors in the parameters of interest.

Following the method of development of reference 1, the expression for enthalpy is found by considering enthalpy as a function of density and temperature

$$dh = \left(\frac{\partial h}{\partial \rho}\right)_T d\rho + \left(\frac{\partial h}{\partial T}\right)_\rho dT \tag{8}$$

Introducing the combined first and second law equation of thermodynamics in the form

$$dh = T\,ds + \frac{1}{\rho}\,dp \tag{9}$$

which can be rewritten for a constant temperature as

$$\left(\frac{\partial h}{\partial \rho}\right)_T = T\left(\frac{\partial s}{\partial \rho}\right)_T + \frac{1}{\rho}\left(\frac{\partial p}{\partial \rho}\right)_T \tag{10}$$

and for a constant density as

$$\left(\frac{\partial h}{\partial T}\right)_\rho = T\left(\frac{\partial s}{\partial T}\right)_\rho + \frac{1}{\rho}\left(\frac{\partial p}{\partial T}\right)_\rho \tag{11}$$

equation (8) may be expressed as

$$dh = \left[-\frac{T}{\rho^2}\left(\frac{\partial p}{\partial T}\right)_\rho + \frac{1}{\rho}\left(\frac{\partial p}{\partial \rho}\right)_T\right] d\rho + \left[c_v + \frac{1}{\rho}\left(\frac{\partial p}{\partial T}\right)_\rho\right] dT \tag{12}$$

by noting, from the Maxwell relation, that

$$T\left(\frac{\partial s}{\partial \rho}\right)_T = -\frac{T}{\rho^2}\left(\frac{\partial p}{\partial T}\right)_\rho \tag{13}$$

and

$$T\left(\frac{\partial s}{\partial T}\right)_\rho = c_v \tag{14}$$

The pressure p is eliminated from equation (12) by use of equation (1). Direct differentiation of equation (1) gives

$$\left(\frac{\partial p}{\partial T}\right)_\rho = \rho R\left\{1 + \rho\left[B(T) + T\,\frac{dB(T)}{dT}\right] + \rho^2\left[C(T) + T\,\frac{dC(T)}{dT}\right] + \rho^3\left[D(T) + T\,\frac{dD(T)}{dT}\right]\right\} \tag{15}$$

and

$$\left(\frac{\partial p}{\partial \rho}\right)_T = RT\left[1 + 2\rho B(T) + 3\rho^2 C(T) + 4\rho^3 D(T)\right] \tag{16}$$

These two equations are now substituted into equation (12), and equation (12), which is an exact differential, may be integrated over a two-step path by first holding ρ constant and integrating with respect to T and then holding T constant and integrating with respect to ρ. When integrating from a reference temperature to a desired temperature for a constant density, the density level chosen can be made as small as desired ($\rho \to 0$)

so that the value of c_v in equation (12) may be set equal to its ideal-gas value of $\frac{3}{2}R$ and $\int \frac{1}{\rho}\left(\frac{\partial p}{\partial T}\right)_\rho dT = RT$. The second integration is performed for a constant desired temperature from this very low reference density up to the desired density. The reference value of the enthalpy (constant of integration) is eliminated by the reference-temperature term since the reference conditions correspond to ideal-gas behavior; that is, $h = \frac{5}{2}RT$ for $\rho \to 0$. Upon integration of equation (12), the expression for enthalpy as a function of ρ and T becomes

$$h = RT\left\{\frac{5}{2} + \rho\left[B(T) - T\frac{dB(T)}{dT}\right] + \frac{\rho^2}{2}\left[2C(T) - T\frac{dC(T)}{dT}\right] + \frac{\rho^3}{3}\left[3D(T) - T\frac{dD(T)}{dT}\right]\right\} \tag{17}$$

where the virial coefficients $B(T)$, $C(T)$, and $D(T)$ are given in equations (7), (4), and (5), respectively. Since the virial coefficients are functions only of the temperature, the derivatives as required in equation (17) can be obtained by direct differentiation.

The expression for entropy as a function of ρ and T is found by considering

$$ds = \left(\frac{\partial s}{\partial \rho}\right)_T d\rho + \left(\frac{\partial s}{\partial T}\right)_\rho dT \tag{18}$$

which can be rewritten, by using equations (13) and (14), as

$$ds = -\frac{1}{\rho^2}\left(\frac{\partial p}{\partial T}\right)_\rho d\rho + \frac{c_v}{T} dT \tag{19}$$

The pressure dependence is eliminated by using equation (15). By integrating over the same two paths for which the enthalpy was determined and noting that the reference value of the entropy (constant of integration) is eliminated at the reference conditions, the expression for entropy as a function of ρ and T becomes

$$s = R\left\{\frac{3}{2}\ln T - \ln \rho - \rho\left[B(T) + T\frac{dB(T)}{dT}\right] - \frac{\rho^2}{2}\left[C(T) + T\frac{dC(T)}{dT}\right] - \frac{\rho^3}{3}\left[D(T) + T\frac{dD(T)}{dT}\right]\right\} \tag{20}$$

The expression for c_v can be determined from equations (14) and (20) and is

$$c_v = \frac{3}{2}R - RT\left\{\rho\left[2\frac{dB(T)}{dT} + T\frac{d^2B(T)}{dT^2}\right] + \frac{\rho^2}{2}\left[2\frac{dC(T)}{dT} + T\frac{d^2C(T)}{dT^2}\right] + \frac{\rho^3}{3}\left[2\frac{dD(T)}{dT} + T\frac{d^2D(T)}{dT^2}\right]\right\} \tag{21}$$

The expression for the speed of sound is found by beginning with the relations

$$a^2 = \left(\frac{\partial p}{\partial \rho}\right)_s = \frac{c_p}{c_v}\left(\frac{\partial p}{\partial \rho}\right)_T \tag{22}$$

$$\frac{c_p}{c_v} = -\frac{T}{c_v \rho^2}\left(\frac{\partial p}{\partial T}\right)_\rho \left(\frac{\partial \rho}{\partial T}\right)_p + 1 \tag{23}$$

$$\left(\frac{\partial p}{\partial \rho}\right)_T = -\left(\frac{\partial p}{\partial T}\right)_\rho \left(\frac{\partial T}{\partial \rho}\right)_p \tag{24}$$

Multiplying equation (23) by equation (24) and substituting the product into equation (22) yields

$$a^2 = \left(\frac{\partial p}{\partial \rho}\right)_T + \frac{T}{c_v \rho^2}\left(\frac{\partial p}{\partial T}\right)_\rho^2 \tag{25}$$

where the two quantities, $\left(\frac{\partial p}{\partial T}\right)_\rho$ and $\left(\frac{\partial p}{\partial \rho}\right)_T$, are given by equations (15) and (16), respectively.

The expression for c_p can be found from equations (23) and (24) in the form

$$c_p = c_v + \frac{\frac{T}{\rho^2}\left(\frac{\partial p}{\partial T}\right)_\rho^2}{\left(\frac{\partial p}{\partial \rho}\right)_T} \tag{26}$$

where $(\partial p/\partial T)_\rho$ and $(\partial p/\partial \rho)_T$ are given by equations (15) and (16), respectively, and c_v has been determined previously from equation (21).

CALCULATION OF FLOW PARAMETERS

The previously derived equations for enthalpy, entropy, speed of sound, and specific heats are used, in conjunction with the equation of state, to provide expressions for determining reservoir, nozzle-throat, test-section free-stream, and test-section normal-shock conditions in real helium for reservoir temperatures from 200° to 15 000° K and reservoir pressures from 1 to 3600 atmospheres (1 atmosphere = 0.101 MN/m^2).

The following procedure for determining various thermodynamic and gas dynamic flow parameters was derived primarily to meet the needs of hotshot-type wind tunnels where, in many instances, the only direct measurements made to define the flow conditions are reservoir pressure after arc discharge and test-section stagnation pressure behind a normal shock. These measured pressures and the initial reservoir density before arc discharge are the basic input data. This procedure is based on the assumptions of the existence of uniform density throughout the reservoir during a tunnel test and an isentropic, one-dimensional flow expansion. The assumption of uniform reservoir density can be avoided by providing an additional measured quantity as input to the calculation procedure. Hence, three possible measured third inputs (free-stream density ρ_∞, free-stream velocity U_∞, and reservoir temperature $T_{t,1}$) are also considered in the following calculation procedure.

The following derived method for calculating reservoir, nozzle-throat, test-section free-stream, and test-section normal-shock conditions was programed for an electronic data processing system. The Newton-Raphson iteration method was employed to solve single equations and simultaneous equations where the initial conditions required for this iteration method were those for an ideal gas.

Before the discussion of the calculation procedure for determining various flow parameters, a brief description of the Langley hotshot tunnel is given. The major components of this facility include a capacitor bank, an arc chamber incorporating coaxial electrodes, a conical nozzle and test section, and a vacuum reservoir. The operating procedure begins by charging (pressurizing) the arc chamber at ambient temperature with the test gas (helium or nitrogen). A quantity of stored electrical energy in the capacitor bank is then discharged across the coaxial electrodes. The resulting increase in pressure and temperature of the gas within the arc chamber results in the rupture of a diaphragm between the arc chamber and evacuated nozzle. The gas then expands through the conical nozzle into the vacuum reservoir. A more detailed description of this facility is presented in reference 8.

Initial Reservoir Conditions

The initial reservoir density before arc discharge is found by using equation (1) in the form

$$\frac{p_c}{RT_c} = \rho_c + \rho_c{}^2 B(T_c) + \rho_c{}^3 C(T_c) + \rho_c{}^4 D(T_c) \tag{27}$$

where the charge pressure p_c is a measured quantity and the charge temperature T_c has been experimentally found to become ambient shortly after charging the reservoir. The parameters B, C, and D are the virial coefficients (eqs. (7), (4), and (5)) and are functions only of charge temperature.

Reservoir Conditions After Arc Discharge

At a tunnel run time of zero (immediately after arc discharge), the reservoir density is equal to the initial reservoir charge density, that is, $(\rho_{t,1})_{\tau=0} = \rho_c$. It is assumed that no density gradients exist in the reservoir at any time after arc discharge. With the reservoir density and measured reservoir pressure known, the reservoir temperature for $\tau = 0$ can be calculated by using equation (1), in which the virial coefficients are functions of the reservoir temperature for $\tau = 0$. Having determined the reservoir density and temperature, the reservoir compressibility factor, enthalpy, entropy, specific heat at constant volume, speed of sound, and specific heat at constant pressure can be calculated directly from equations (2), (17), (20), (21), (25), and (26), respectively.

For $\tau > 0$, the time-monitored reservoir pressure is known, but the stagnation density has decreased from the value for $\tau = 0$ as a result of the mass flow from the

reservoir. To account for this time variation in stagnation density, it is necessary to calculate the mass flow from the reservoir (discussed in the following section) and adjust the reservoir density accordingly.

Nozzle-Throat Conditions

As mentioned previously, it is necessary to determine the mass flow from the reservoir through the nozzle throat as a function of tunnel run time. The relationships necessary for determining the mass flow from the reservoir through the nozzle throat are derived by assuming isentropic flow

$$s^*(\rho^*,T^*) = s_{t,1} \tag{28}$$

and noting that the Mach number at the nozzle throat M^* is unity; that is, the speed of sound at the nozzle throat is equal to the velocity at the nozzle throat ($a^* = U^*$). The energy equation

$$U^2 = 2(h_{t,1} - h) \tag{29}$$

is considered in conjunction with $a^* = U^*$ to yield the expression

$$h^*(\rho^*,T^*) + \frac{1}{2}\left[a^*(\rho^*,T^*)\right]^2 = h_{t,1} \tag{30}$$

where the reservoir enthalpy $h_{t,1}$ has been calculated previously, h^* is given by equation (17) as a function of ρ^* and T^*, and $(a^*)^2$ is given by equation (25) also as a function of ρ^* and T^*. Since $s_{t,1}$ has been calculated previously and s^* is given by equation (20) as a function of ρ^* and T^*, equations (28) and (30) can be solved simultaneously for ρ^* and T^*. With ρ^* and T^* determined, h^* may be calculated directly from equation (17) and U^* from equation (29).

The reservoir density can now be adjusted (adjustment is required due to mass flow from the reservoir with tunnel run time) by the equation

$$(\rho_{t,1})_{\tau_{present}} = (\rho_{t,1})_{\tau_{previous}} - \rho^* U^* \frac{\pi(d^*)^2 \Delta\tau}{4V} \tag{31}$$

where the nozzle-throat diameter d^* and reservoir volume V are geometric input parameters and $\Delta\tau$ represents the desired time increment. Depending on the rate of mass flow from the reservoir through the nozzle throat, the time increments of equation (31) should be chosen small enough so that a further decrease in $\Delta\tau$ does not result in significant variations in $\rho_{t,1}$ for all τ (larger mass flow rates require smaller time increments).

The determination of the reservoir density, hence reservoir temperature, enthalpy, and so forth, as a function of tunnel run time is best illustrated by an example. Assume that $p_{t,1}$ has been measured at 0.005-sec intervals, beginning immediately after arc

discharge ($\tau = 0$), so that $\tau_0 = 0$, $\tau_1 = 0.005$ sec, $\tau_2 = 0.010$ sec, ... For $\tau_0 = 0$, $\rho_{t,1} = \rho_c$, thereby permitting calculation of $T_{t,1}$, $h_{t,1}$, $s_{t,1}$, and so forth, at τ_0. Since only the measured quantity $p_{t,1}$ is known at τ_1, $\rho_{t,1}$ at τ_1 is found by subtracting the mass flow from the reservoir over the time increment $\tau_1 - \tau_0$ from the previously calculated value of $\rho_{t,1}$ at τ_0. This is accomplished by first calculating ρ^* and T^* from the simultaneous solution of equations (28) and (30) where $h_{t,1}$ and $s_{t,1}$ correspond to τ_0. The nozzle-throat velocity U^* is calculated from equation (29), where $h_{t,1}$ and h^* correspond to τ_0, and equation (31) becomes

$$\left(\rho_{t,1}\right)_{\tau_1}^{(1)} = \left(\rho_{t,1}\right)_{\tau_0} - \left(\rho^* U^*\right)_{\tau_0} \frac{\pi (d^*)^2 (\tau_1 - \tau_0)}{4V}$$

This value of $\left(\rho_{t,1}\right)_{\tau_1}^{(1)}$ is the first approximation (indicated by superscript (1)) of $\rho_{t,1}$ at τ_1. By using $\left(\rho_{t,1}\right)_{\tau_1}^{(1)}$ in conjunction with the measured value of $\left(p_{t,1}\right)_{\tau_1}$, the parameters $T_{t,1}$, $h_{t,1}$, $s_{t,1}$, ρ^*, and U^* can be calculated at τ_1 and a new value of $\rho_{t,1}$ at τ_1 can be found from

$$\left(\rho_{t,1}\right)_{\tau_1}^{(2)} = \left(\rho_{t,1}\right)_{\tau_0} - \left(\rho^* U^*\right)_{\tau_1}^{(1)} \frac{\pi (d^*)^2 (\tau_1 - \tau_0)}{4V}$$

where $\left(\rho_{t,1}\right)_{\tau_1}^{(2)}$ is the second approximation of $\rho_{t,1}$ at τ_1 and $\left(\rho^* U^*\right)_{\tau_1}^{(1)}$ corresponds to the first approximation of $\rho_{t,1}$ at τ_1 obtained from the preceding equation. If this new value of $\rho_{t,1}$ at τ_1 $\left(\text{that is, } \left(\rho_{t,1}\right)_{\tau_1}^{(2)}\right)$ is within the desired accuracy (0.01 percent for the present study) of the previous value of $\rho_{t,1}$ at τ_1 $\left(\text{that is, } \left(\rho_{t,1}\right)_{\tau_1}^{(1)}\right)$ the calculated parameters corresponding to the new value of $\rho_{t,1}$ at τ_1 are considered satisfactory; if not, this procedure must be repeated until the desired accuracy is obtained. The nozzle-throat pressure p^* at τ_1 can be calculated directly from equation (1) since ρ^* and T^* at τ_1 are now known.

Free-Stream Conditions

For $M_\infty > 10$, the free-stream enthalpy is less than about 3 percent of the reservoir enthalpy. Therefore, the free-stream velocity can be approximated by allowing $h_\infty = 0$ in equation (29), which gives

$$\tilde{U}_\infty^2 = 2h_{t,1} \tag{32}$$

The ratio of the free-stream dynamic pressure to reservoir pressure for isentropic flow of an ideal gas is given in reference 9 as

$$\frac{q_\infty}{p_{t,1}} = \frac{\gamma}{2} M_\infty{}^2 \left(1 + \frac{\gamma - 1}{2} M_\infty{}^2\right)^{-\frac{\gamma}{\gamma-1}} \tag{33}$$

Also from reference 9, the ratio of total pressure behind a normal shock to reservoir pressure for adiabatic flow of an ideal gas is given by

$$\frac{p_{t,2}}{p_{t,1}} = \left[\frac{(\gamma + 1)M_\infty{}^2}{(\gamma - 1)M_\infty{}^2 + 2}\right]^{\frac{\gamma}{\gamma-1}} \left[\frac{\gamma + 1}{2\gamma M_\infty{}^2 - (\gamma - 1)}\right]^{\frac{1}{\gamma-1}} \tag{34}$$

Dividing equation (33) by equation (34) and noting that $q_\infty = \frac{1}{2}\rho_\infty U_\infty{}^2$ results in the following equation for free-stream density:

$$\tilde{\rho}_\infty = \frac{2p_{t,2}}{U_\infty{}^2}\left(\frac{4}{\gamma}\right)^{\frac{1}{\gamma-1}}\left(\frac{\gamma}{\gamma+1}\right)^{\frac{\gamma+1}{\gamma-1}}\left(1 - \frac{\gamma - 1}{2\gamma}\frac{1}{M_\infty{}^2}\right)^{\frac{1}{\gamma-1}} \tag{35}$$

Since $M_\infty{}^2 >> 1$ for the present study, equation (35) can be simplified to

$$\tilde{\rho}_\infty \approx \Gamma(\gamma)\frac{p_{t,2}}{U_\infty{}^2} \tag{36}$$

where

$$\Gamma(\gamma) = 2\left(\frac{4}{\gamma}\right)^{\frac{1}{\gamma-1}}\left(\frac{\gamma}{\gamma+1}\right)^{\frac{\gamma+1}{\gamma-1}}$$

and $\Gamma(\gamma)$ is equal to 1.1347 for ideal helium ($\gamma = 1.6667$). A superscript ($\sim$) on ρ_∞ indicates an approximate value since equation (36) was obtained from ideal-gas relations. Equation (36) thus provides an approximation of the free-stream density based on the measured total pressure behind a normal shock and estimated free-stream velocity as determined from equation (32).

From the assumption $s_{t,1} = s_\infty$, and with $\tilde{\rho}_\infty$ known, T_∞ can be calculated numerically from equation (20). Free-stream pressure p_∞ and free-stream enthalpy h_∞ can then be determined directly from equations (1) and (17), respectively.

Since $\tilde{U}_\infty$ represents an approximation of the free-stream velocity due to the omission of the free-stream enthalpy contribution, free-stream velocity can now be calculated from equation (29) in the form

$$U_\infty{}^2 = 2\left(h_{t,1} - h_\infty\right)$$

By using this value of U_∞, a new value of $\tilde{\rho}_\infty$ and hence of T_∞ and h_∞ can be calculated, thus leading to a second new value of U_∞. This procedure is repeated until the desired accuracy between successive values of U_∞ (0.01 percent for the present study)

is obtained. The free-stream parameters $(\tilde{\rho}_\infty, T_\infty)$ corresponding to the final value of free-stream velocity in this iteration can now be used to calculate the free-stream speed of sound a_∞ from equation (25). The free-stream Mach number M_∞ is simply found by dividing U_∞ by a_∞, and the free-stream dynamic pressure is found from $q_\infty = \frac{1}{2}\tilde{\rho}_\infty U_\infty^2$. The values of Z_∞, $c_{v,\infty}$, and $c_{p,\infty}$ are calculated directly from equations (2), (21), and (26), respectively, and the free-stream ratio of specific heats is found from $\gamma_\infty = \frac{c_{p,\infty}}{c_{v,\infty}}$. The free-stream coefficient of viscosity μ_∞ is given to within 1 percent for the temperature range 4° to 1100° K by the empirical expression (ref. 10)

$$\mu_\infty = \left(1.2548 \times 10^{-6}\right) T_\infty^{0.647} \tag{37}$$

where μ_∞ is in moles/cm-sec for T_∞ in $^\circ$K. The experimental viscosity results collected in reference 10 show that for a temperature of 1.64° K, the value of μ calculated from equation (37) is 1.255 times the experimental value. However, it should be pointed out that this is the only available experimental result for temperatures less than 4° K. In the absence of stronger evidence of error, equation (37) is employed in this study for $T_\infty < 4^\circ$ K. The free-stream Reynolds number, per unit length, is found by dividing the product $\tilde{\rho}_\infty U_\infty$ by μ_∞. The ratio of effective nozzle-throat area to effective nozzle-test-section area is obtained from the equation of continuity

$$\frac{A^*}{A} = \frac{\tilde{\rho}_\infty U_\infty}{\rho^* U^*} \tag{38}$$

In order to calculate these free-stream conditions, the free-stream velocity and density were approximated from equations (32) and (36), respectively. Although the inaccuracy in approximating free-stream velocity was eliminated in this section by an iterative procedure, the free-stream density is still an approximation since equation (36) was derived by using ideal-gas relations. The validity of this value of $\tilde{\rho}_\infty$ is examined in a subsequent section.

In the calculation of these free-stream conditions, the real-helium expressions developed in a previous section "Basic Thermodynamic Relations" were used. For the present range of reservoir conditions and Mach number, the free-stream temperature range is approximately 1.0° to 440° K and the maximum free-stream density is approximately 1.2×10^{-4} mole/cm^3. Due to this low range of free-stream density, terms appearing in equation (2) which involve $C(T)$ and $D(T)$ are essentially negligible in the free stream. The use of equation (7) for determining $B(T)$ at free-stream temperatures less than 200° K is questionable. (See fig. 1.) For the most unfavorable conditions, the use of equation (7) results in a value of Z_∞ which is approximately 1.003 times the more correct value obtained from the experimental values of $B(T)$ tabulated in reference 10 for very low temperatures. By allowing $B(T_\infty) = 0$ for $T_\infty < 200^\circ$ K, this discrepancy in Z_∞ is reduced to approximately 1.001; therefore, in the present method, $B(T_\infty)$, $C(T_\infty)$, and $D(T_\infty)$ were set equal to zero when $T_\infty < 200^\circ$ K.

An item of concern in the free-stream flow of a gas is that of flow condensation. To determine whether helium condensation might be present in the free stream, the following empirical expressions from reference 10 are included in the present method. For $T_\infty \geq 2.190^\circ$ K

$$\log_{10} p_{con} = -\frac{3.024}{T_\infty} + 2.208 \log_{10} T_\infty - 0.664 \tag{39a}$$

and for $T_\infty < 2.190^\circ$ K

$$\log_{10} p_{con} = -\frac{3.859}{T_\infty} + 0.922 \log_{10} T_\infty + 0.154 \tag{39b}$$

where p_{con} is in atmospheres for T_∞ in $^\circ$K. If the free-stream pressure p_∞ is less than the calculated condensation pressure p_{con}, condensation will not be expected to occur; however, if $p_\infty \geq p_{con}$, condensation may occur.

Static Conditions Behind Normal Shock

The conservation relations for mass, momentum, and energy across a normal shock are

$$\rho_\infty U_\infty = \rho_2 U_2 \tag{40}$$

$$p_\infty + \rho_\infty U_\infty^2 = p_2 + \rho_2 U_2^2 \tag{41}$$

and

$$h_{t,1} = h_\infty + \frac{1}{2} U_\infty^2 = h_2 + \frac{1}{2} U_2^2 \tag{42}$$

From equations (1), (40), and (41) the expression

$$p_\infty + \rho_\infty U_\infty^2 = \rho_2 R T_2 \left[1 + \rho_2 B(T_2) + \rho_2^2 C(T_2) + \rho_2^3 D(T_2)\right] + \frac{(\rho_\infty U_\infty)^2}{\rho_2} \tag{43}$$

can be obtained. Similarly, from equations (17), (40), and (42) the expression

$$h_{t,1} = R T_2 \left\{ \frac{5}{2} + \rho_2 \left[B(T_2) - T_2 \frac{dB(T_2)}{dT_2} \right] + \frac{\rho_2^2}{2} \left[2C(T_2) - T_2 \frac{dC(T_2)}{dT_2} \right] \right.$$

$$\left. + \frac{\rho_2^3}{3} \left[3D(T_2) - T_2 \frac{dD(T_2)}{dT_2} \right] \right\} + \frac{1}{2} \left(\frac{\rho_\infty U_\infty}{\rho_2} \right)^2 \tag{44}$$

can be obtained. Equations (43) and (44) can be solved simultaneously for ρ_2 and T_2. With ρ_2 and T_2 known, the parameters p_2, h_2, s_2, a_2, $c_{v,2}$, $c_{p,2}$, γ_2, and Z_2 can be calculated directly.

At this point in the calculation procedure, the value of free-stream density used in the calculation of free-stream conditions and static conditions behind a normal shock is an approximate value since equation (36) was derived by using ideal-gas relations. It is now possible to examine the validity of this value of free-stream density. The variation in conditions from immediately downstream of the shock to the stagnation point is relatively small, and the level of density in this region is also relatively small for the present range of reservoir conditions and free-stream Mach number (approximately 4 times the maximum free-stream density). Thus, this region may be considered to behave as an ideal gas and must satisfy the condition $s_2 = s_{t,2}$. Now p_2 can be calculated from the ideal-gas isentropic relation (ref. 9)

$$p_2 = p_{t,2}\left(1 + \frac{\gamma_2 - 1}{2} M_2^2\right)^{-\frac{\gamma_2}{\gamma_2 - 1}} \tag{45}$$

where $p_{t,2}$ is the measured stagnation pressure behind a normal shock. This value of p_2 is compared with the value of p_2 obtained previously, and if these values are not within the desired accuracy (0.01 percent for the present study), a new value of ρ_∞ is determined from the relation

$$(\rho_\infty)_{new} = \tilde{\rho}_\infty\left(\frac{p_2'}{p_2}\right) \tag{46}$$

where p_2' denotes the value of p_2 obtained from equation (45). The calculation procedure, beginning immediately after equation (36), where $\tilde{\rho}_\infty = (\rho_\infty)_{new}$, is repeated until the desired accuracy is obtained.

Stagnation Conditions Behind Normal Shock

The stagnation conditions behind a normal shock must satisfy the condition $h_{t,2} = h_{t,1}$. Thus, equation (17) can be expressed as a function of $\rho_{t,2}$ and $T_{t,2}$. Since $p_{t,2}$ is a measured quantity, equation (1) can also be expressed as a function of $\rho_{t,2}$ and $T_{t,2}$. After $\rho_{t,2}$ and $T_{t,2}$ have been obtained from the simultaneous solution of equations (1) and (17), the parameters $s_{t,2}$, $(c_v)_{t,2}$, $(c_p)_{t,2}$, $\gamma_{t,2}$, and $Z_{t,2}$ can be calculated directly. Equation (37) can be used to calculate $\mu_{T,2}$ for values of $T_{t,2}$ less than 1100° K. To obtain an expression for $\mu_{t,2}$ for values of $T_{t,2}$ greater than 1100° K, a manual adjustment was made on equation (37) to obtain better agreement with results of reference 7; the resulting equation is

$$\mu_{t,2} \approx \left(1.2548 \times 10^{-6}\right) T_{t,2}^{0.647} \exp\left[\left(6.04 \times 10^{-5}\right) T_{t,2} - \left(0.23 \times 10^{-8}\right) T_{t,2}^2\right] \tag{47}$$

where $\mu_{t,2}$ is in moles/cm-sec for $T_{t,2}$ in ^{o}K. For values of $T_{t,2}$ less than 1625^{o} K, equation (37) predicts $\mu_{t,2}$ within 4 percent of the results of reference 7, whereas for values of $T_{t,2}$ between 1625^{o} and $11\ 000^{o}$ K, equation (47) yields values of $\mu_{t,2}$ within 4 percent.

Procedure Using an Additional Experimental Input

The previously discussed procedure for determining various flow parameters was derived for the case when only reservoir pressure and stagnation pressure behind a normal shock are measured to define the flow. This procedure was based on the assumption that uniform density existed throughout the reservoir. The validity of this assumption is questionable in explosive arc-heated facilities, and this assumption can be avoided by measuring one other flow parameter in conjunction with the measured pressures. (It is assumed that simultaneous measurements of reservoir pressure, stagnation pressure behind a normal shock, and the third flow parameter are made throughout the test.)

Free-stream density.- Successful free-stream density measurements have recently been made in the Langley hotshot tunnel by using an electron beam in nitrogen flow. If the electron-beam technique proves to be applicable for measuring free-stream densities in helium, this measurement can be utilized as an additional input. The calculation procedure for determining the various flow parameters of interest when free-stream density is a measured quantity begins by combining equations (32) and (36) to form

$$h_{t,1} \approx \frac{1}{2}\,\Gamma(\gamma)\frac{p_{t,2}}{\rho_{\infty}} \tag{48}$$

where $p_{t,2}$ is also a measured quantity and h_{∞} has been neglected. This calculated value of reservoir enthalpy can be used in equation (17), thereby expressing equation (17) in terms of reservoir density and temperature. Since reservoir pressure is a measured quantity, equation (1) can also be expressed in terms of reservoir density and temperature. Equations (1) and (17) can then be solved simultaneously for $\rho_{t,1}$ and $T_{t,1}$. When these reservoir parameters and, of course, $p_{t,2}$ are known, the remaining phase of the calculation procedure is the same as discussed previously, except that the mass-flow iterative procedure (eq. (31)) is no longer necessary. Since equation (48) is only an approximation of the reservoir stagnation enthalpy, the final calculated value of ρ_{∞} is compared with the measured value of ρ_{∞}. If these values are not within the desired accuracy (0.01 percent for the present study), the reservoir density corresponding to the final calculated free-stream density is adjusted by use of the relation

$$(\rho_{t,1})_{new} = \frac{(\rho_{t,1})_{calc}(\rho_{\infty})_{m}}{(\rho_{\infty})_{calc}} \tag{49}$$

This new value of reservoir density is introduced into equation (1) in order to calculate a new value of reservoir temperature. The calculation procedure is repeated with these new values of $\rho_{t,1}$ and $T_{t,1}$, and a second comparison of the final calculated free-stream density, corresponding to these new values of $\rho_{t,1}$ and $T_{t,1}$, is made with the measured free-stream density. This procedure is repeated until the desired accuracy is obtained.

Free-stream velocity.- Measurements of free-stream velocity have been performed in the Langley hotshot tunnel by photographically observing the travel of spark discharges in the nitrogen flow stream. It is believed that this technique may also be applicable for determining free-stream velocities in helium. The calculation procedure for determining the various flow parameters of interest when free-stream velocity is a measured quantity begins by estimating the reservoir enthalpy from equation (32) where h_∞ is neglected for the time being. With $h_{t,1}$ (approximately) and $p_{t,1}$ known, equations (1) and (17) can be solved simultaneously for $\rho_{t,1}$ and $T_{t,1}$. The remaining reservoir and nozzle-throat conditions can be calculated as discussed previously, again noting that the mass-flow iterative procedure (eq. (31)) is no longer necessary. The final value of free-stream velocity calculated from equation (29), where the contribution of h_∞ is included, is compared with the measured value of free-stream velocity. If these values are not within the desired accuracy (0.01 percent for the present study), the left side of equation (17) is set equal to $\frac{(U_\infty)_m^2}{2} + h_\infty$, where the value of h_∞ is that corresponding to the final calculated free-stream velocity. Thus, a second final value of free-stream velocity can be calculated and compared with the measured free-stream velocity. This procedure is repeated until the desired accuracy is obtained.

Reservoir temperature.- The present technique for measuring reservoir temperature in hotshot tunnels is not fully developed because of the severity of the arc-chamber conditions. Nevertheless, the continuous measurement of reservoir temperature is also considered as an additional input. The calculation procedure is then very similar to that discussed previously when only $p_{t,1}$ and $p_{t,2}$ are measured inputs, the only difference being that the reservoir density can now be calculated directly by the use of equation (1). Therefore, the mass-flow iterative procedure (eq. (31)) is no longer necessary.

Hypothetical case using free-stream Mach number as an input.- Calculations of a number of hypersonic nozzle flow parameters for real helium have been performed and presented in reference 1 in the form of simple correction factors for reservoir pressures to 3400 atmospheres, temperatures to 5800° K, and free-stream Mach numbers to 100. The results of reference 1 were obtained by using the Beattie-Bridgeman equation of state, for which the constants used were determined from experimental data for temperatures to only 590° K. In order to obtain more accurate real-helium effects at

temperatures above 590° K, the present method based on the virial equation of state was used to determine the flow properties of real helium by using free-stream Mach number as an input along with reservoir pressure and temperature. The purpose of this hypothetical calculation procedure is to obtain simple correction factors in the form of ratios of a real-helium value of a particular flow parameter to its ideal-helium value and to present these correction factors in working charts.

The calculation procedure for determining reservoir and nozzle-throat conditions when reservoir pressure and temperature are inputs has been discussed previously. The free-stream conditions are determined by first estimating U_∞ by using equation (32), where h_∞ is neglected, and considering the relation

$$\left[a_\infty\left(\rho_\infty, T_\infty\right)\right]^2 = \frac{\tilde{U}_\infty{}^2}{M_\infty{}^2} \tag{50}$$

where $a_\infty{}^2$ is given by equation (25) and the right side of equation (50) is known. From the assumption of isentropic flow $\left(s_\infty\left(\rho_\infty, T_\infty\right) = s_{t,1}\right)$, equations (20) and (50) can be solved simultaneously for ρ_∞ and T_∞; thereby, the use of equation (36) and hence of equations (45) and (46) is avoided. The free-stream enthalpy can be calculated directly from equation (17) and a new value of U_∞ can be found from equation (29). This new value of U_∞ is compared with the previously calculated value of U_∞. If these values of U_∞ are not within the desired accuracy of each other (0.01 percent for the present study), the new value of U_∞ is placed into equation (50) and this procedure is repeated until the desired accuracy between successive values of U_∞ is obtained. With ρ_∞ and T_∞ known, the various free-stream parameters of interest can be calculated. The static conditions behind a normal shock can be determined as discussed previously. The stagnation conditions behind a normal shock must satisfy the conditions $h_{t,2}\left(\rho_{t,2}, T_{t,2}\right) = h_{t,1}$ and $s_{t,2}\left(\rho_{t,2}, T_{t,2}\right) = s_2$, where $h_{t,1}$ and s_2 have been determined previously. Thus, equations (17) and (20) can be solved simultaneously for $\rho_{t,2}$ and $T_{t,2}$ and $p_{t,2}$ can be determined from equation (1). The results of this hypothetical calculation procedure are restricted to reservoir densities less than 0.0173 mole/cm^3, the critical density of helium, and to uncondensed free-stream flow as defined by equation (39).

RESULTS AND DISCUSSION

The results of the calculations for helium based on the virial form of the equation of state where free-stream Mach number was used as an input along with reservoir pressure and temperature are shown in figures 2, 3, 4, and 5. Various reservoir and nozzle-throat thermodynamic parameters are plotted in figures 2 and 3, respectively, as a function of reservoir pressure to 3600 atmospheres for reservoir temperatures ranging from 200° to 15 000° K. The ideal-gas value of a particular reservoir or nozzle-throat

thermodynamic parameter is shown in figures 2 and 3 where appropriate. (The ideal-gas expressions of ref. 11 are shown in fig. 3.) The results of figures 2 and 3 are restricted to reservoir densities less than the critical density of helium.

Figure 4 shows the results of the calculations in the form of correction factors to be used in conjunction with the ideal-gas parameters for helium presented in references 12 and 13. These correction factors are ratios of real-to-ideal flow parameters and are plotted in figure 4 as functions of reservoir pressure to 3600 atmospheres for reservoir temperatures ranging from 200° to 15 000° K and a range of Mach numbers from 10 to 100. The Mach number ratio of figure 4(a) represents the real-helium, or input, Mach number divided by the ideal-helium Mach number as determined from equation (34), where $p_{t,2}/p_{t,1}$ is a real-helium quantity ($p_{t,1}$ is an input parameter and $p_{t,2}$ corresponds to input Mach number) and $\gamma = 5/3$. As in reference 1, the real-helium flow parameters of figures 4(b) to 4(f) are divided by the corresponding ideal-gas flow parameter (obtained from refs. 12 or 13) for the same value of M_∞ to give the correction factors. The results of figure 4 are restricted to reservoir densities less than the critical density of helium and to Mach numbers corresponding to uncondensed flow.

The use of the correction factors presented in figure 4 is essentially the same as discussed in reference 1 except that no iterative procedure is required for the determination of the real-helium Mach number. For example, assume that a hypersonic helium tunnel operates with $p_{t,1} = 1000$ atm, $T_{t,1} = 900°$ K, and $p_{t,2} = 0.9533$ atm. From figure 4(a), these conditions correspond to $\frac{M_\infty}{(M_\infty)_i} = 1.0429$, and for $\frac{p_{t,2}}{p_{t,1}} = 0.9533 \times 10^{-3}$, reference 12 yields $(M_\infty)_i = 28.77$; therefore, M_∞ is determined by multiplying the ideal-gas value of Mach number as found in reference 12 by the correction factor 1.0429 and is found to be equal to 30. Once the value of M_∞ has been determined, other corresponding ideal-gas flow parameters can be found from the tables of reference 12 ($1 \leq M_\infty \leq 40$) or reference 13 ($40 \leq M_\infty \leq 100$). For instance, for $M_\infty = 30$, reference 12 shows that $\left(\frac{p_\infty}{p_{t,1}}\right)_i = 0.6362 \times 10^{-6}$ and figure 4(b) shows that for $p_{t,1} = 1000$ atm, $T_{t,1} = 900°$ K, and $M_\infty = 30$, $\frac{p_\infty/p_{t,1}}{(p_\infty/p_{t,1})_i} = 1.1330$; $p_\infty/p_{t,1}$ is found, by multiplying the ideal-gas value by the correction factor, to be 0.7208×10^{-6}; $p_\infty = 0.7208 \times 10^{-3}$ atm. The other flow parameters are determined in the same manner. For Mach numbers between 10 and 30, a Mach number dependency is observed for most of the correction factors; however, for Mach numbers greater than 30, the correction factors are essentially independent of Mach number. The correction factors for p_2/p_∞, ρ_2/ρ_∞, T_2/T_∞, $p_{t,2}/p_\infty$, and M_2 are not presented since they were all within 0.3 percent of unity for a Mach number of 10 and within 0.05 percent of unity for a Mach number of 20 or greater for the entire range of reservoir pressure and temperature. The correction factors for

$q_\infty/p_{t,1}$ and $p_{t,2}/p_{t,1}$ were within 0.05 percent of the correction factor for $p_\infty/p_{t,1}$ for given $p_{t,1}$, $T_{t,1}$, and M_∞ for the entire range of calculation and hence were considered to be equal (fig. 4(b)). To avoid the cross-plotting generally associated with working charts, the correction factors of figures 4(a) to 4(d) were cast into the form of simple equations which are presented in the appendix.

In figure 5, the compressibility factor $Z_{t,1}$ is plotted as a function of reservoir pressure for various reservoir temperatures. The solid lines denote the results of the present calculations based on the virial equation of state, whereas the dash lines denote the results of the calculation procedure of reference 1 which was based on the Beattie-Bridgeman equation of state. The compressibility factor was selected to make a direct comparison between the present calculation procedure and that of reference 1 since it is the governing parameter for real-gas effects in helium. Figure 5 shows that the compressibility factors calculated in reference 1 were always greater than those of the present calculations for a given pressure and temperature. Because of the larger calculated compressibility factors of reference 1 (which imply a greater departure from ideal-gas behavior) the correction factors of reference 1 tend to overcorrect the ideal-gas parameters in comparison with the present correction factors. For example, for $p_{t,1} = 2000$ atm and $T_{t,1} = 1367^\circ$ K, a 5.1 percent discrepancy in $Z_{t,1}$ corresponds to the correction factors for $p_\infty/p_{t,1}$, $\rho_\infty/\rho_{t,1}$, and $T_\infty/T_{t,1}$ of reference 1 being approximately 7.3 percent, 11.4 percent, and 1.9 percent greater, respectively, than those of the present study. The existing discrepancies between the results of the present study and those of reference 1 are not unexpected since, as pointed out in reference 1, the results of reference 1 were obtained by using constants for the Beattie-Bridgeman equation of state which were determined from experimental data for temperatures to only 590° K and thus should be treated as approximations for $T_{t,1} > 590^\circ$ K. Hence, it is believed that a more accurate description of real-helium effects is obtained from the present calculation procedure based on the virial equation of state.

As discussed previously, the expression for free-stream density (eq. (36)) was obtained from ideal-gas relations, thereby making it necessary to examine its validity. This was performed by assuming that the region from immediately downstream of the shock to the stagnation point behaves as an ideal gas and thus allows equation (45) to be employed. The results of the calculations of the hypothetical case (using free-stream Mach number as input), which avoid the use of equation (36), showed that p_2 determined from equation (45) (denoted p_2') was within 0.04 percent of p_2 determined from equation (1) at $M_\infty = 10$ and within 0.005 percent at $M_\infty \geq 20$ for the present range of reservoir pressure and temperature. This supports the validity of equation (45) and hence the use of equation (46) to determine the free-stream density. Calculations for a number of tunnel tests at Mach numbers from approximately 30 to 80 showed that equation (36) is

very accurate, yielding results within 0.3 percent of the final value of ρ_∞ obtained from equation (46) at $M_\infty \approx 30$, with the accuracy improving with increasing Mach number. The accuracy of equation (36) can be attributed to the fact that the ideal-gas relations (eqs. (33) and (34)) used to derive equation (36) have real-helium correction factors within 0.05 percent of one another, for given $p_{t,1}$, $T_{t,1}$, and M_∞, over the present range of calculation.

CONCLUDING REMARKS

The virial form of the equation of state was used to derive a method for determining reservoir, nozzle-throat, free-stream, and normal-shock conditions for real-helium flow. This method was derived primarily to meet the needs of hotshot-type tunnels, where the basic input data are measured reservoir pressure and stagnation pressure behind a normal shock, and was based on the assumption of uniform density throughout the reservoir during a tunnel test. The method was derived with the capability of using an additional measurement of free-stream density, free-stream velocity, or reservoir temperature; this additional measurement as input allows the assumption of uniform density to be avoided. The method was applied for reservoir pressures to 3600 atmospheres, temperatures to 15 000° K, and a range of free-stream Mach numbers from 10 to 100, and the results are presented in the form of nondimensionalized reservoir thermodynamic and nozzle-throat parameters and as simple correction factors which may be applied to ideal-helium flow parameters. The present correction factors were compared with the correction factors of NASA TN D-1632, which were obtained by using the Beattie-Bridgeman equation of state where the constants used were determined from experimental data for temperatures to only 590° K. This comparison showed that the correction factors of NASA TN D-1632 tend to overcorrect the ideal-helium flow parameters. The present calculations are restricted to reservoir densities less than the critical density of helium and to theoretically uncondensed free-stream flow.

Langley Research Center,
National Aeronautics and Space Administration,
Langley Station, Hampton, Va., June 24, 1968,
124-07-02-54-23.

APPENDIX

SIMPLIFIED METHOD FOR DETERMINING REAL-HELIUM HYPERSONIC FLOW PARAMETERS

To provide a rapid determination of various real-helium flow parameters, the correction factors of figures 4(a) to 4(d) were cast into the form of simple equations, and thereby the cross-plotting generally associated with working charts such as figure 4 was avoided.

Except for Mach numbers between 10 and 30, the correction factors were essentially independent of Mach number. Consequently, equations were obtained for each correction factor in terms of reservoir temperature and pressure for $M_\infty \geqq 30$ and $300^\circ\ K \leqq T_{t,1} \leqq 15\ 000^\circ\ K$. The equations are

$$\frac{M_\infty}{(M_\infty)_i} = 1 + p_{t,1}\left(\frac{0.5114}{T_{t,1}^{1.3744}} - \frac{1.1937 \times 10^2}{T_{t,1}^{2.5901}}\right) \tag{51}$$

$$\frac{p_\infty/p_{t,1}}{(p_\infty/p_{t,1})_i} = 1 + p_{t,1}\left(\frac{1.4538}{T_{t,1}^{1.3640}} - \frac{1.3801 \times 10^3}{T_{t,1}^{2.8233}}\right) \tag{52}$$

$$\frac{\rho_\infty/\rho_{t,1}}{(\rho_\infty/\rho_{t,1})_i} = 1 + p_{t,1}\left(\frac{2.5822}{T_{t,1}^{1.3885}} - \frac{2.0911 \times 10^3}{T_{t,1}^{2.8478}}\right) \tag{53}$$

$$\frac{T_\infty/T_{t,1}}{(T_\infty/T_{t,1})_i} = 1 + p_{t,1}\left(\frac{0.7901}{T_{t,1}^{1.3628}} - \frac{2.4311 \times 10^1}{T_{t,1}^{2.1286}}\right) \tag{54}$$

where $p_{t,1}$ is in atmospheres and $T_{t,1}$ is in $^\circ K$. Equations (52) to (54) may be applied for Mach numbers between 20 and 30 with a small uncertainty (less than 0.2 percent at $M_\infty = 20$). Use of these equations for Mach numbers less than 20 will result in correction factors that are as much as 1 percent too large for equations (52) and (53) and 0.5 percent for equation (54) for the present range of reservoir conditions.

REFERENCES

1. Erickson, Wayne D.: An Extension of Estimated Hypersonic Flow Parameters for Helium as a Real Gas. NASA TN D-1632, 1963.

2. Harrison, Edwin F.: Intermolecular-Force Effects on the Thermodynamic Properties of Helium With Application. AIAA J. (Tech Notes), vol. 2, no. 10, Oct. 1964, pp. 1854-1856.

3. Schneider, W. G.; and Duffie, J. A. H.: Compressibility of Gases at High Temperatures. II. The Second Virial Coefficient of Helium in the Temperature Range of 0°C to 600°C. J. Chem. Phys., vol. 17, no. 9, Sept. 1949, pp. 751-754.

4. Yntema, J. L.; and Schneider, W. G.: Compressibility of Gases at High Temperatures. III. The Second Virial Coefficient of Helium in the Temperature Range of 600°C to 1200°C. J. Chem. Phys., vol. 18, no. 5, May 1950, pp. 641-646.

5. Beattie, James A.: Volumetric Behavior and Thermodynamic Properties of the Gas Phase. Argon, Helium, and the Rare Gases, Vol. I, Gerhard A. Cook, ed., Interscience Publ., 1961, pp. 251-312.

6. Michels, A.; and Wouters, H.: Isotherms of Helium Between 0° and 150°C up to 200 Amagat. Physica, vol. VIII, no. 8, Sept. 1941, pp. 923-932.

7. Amdur, I.; and Mason, E. A.: Properties of Gases at Very High Temperatures. Phys. Fluids, vol. 1, no. 5, Sept.-Oct. 1958, pp. 370-383.

8. Miller, Charles G., III.; Creel, Theodore R., Jr.; and Smith, Fred M.: Calibration Experience in the Langley Hotshot Tunnel for Mach Numbers From 12 to 26. NASA TN D-3278, 1966.

9. Ames Research Staff: Equations, Tables, and Charts for Compressible Flow. NACA Rep. 1135, 1953. (Supersedes NACA TN 1428.)

10. Keesom, W. H.: Helium. Elsevier, 1942.

11. Liepmann, H. W.; and Roshko, A.: Elements of Gasdynamics. John Wiley & Sons, Inc., c.1957.

12. Mueller, James N.: Equations, Tables, and Figures for Use in the Analysis of Helium Flow at Supersonic and Hypersonic Speeds. NACA TN 4063, 1957.

13. Mueller, James N.: Ideal-Gas Tables for Helium Flow in the Mach Number Range From 40 to 100. NASA TN D-1252, 1962.

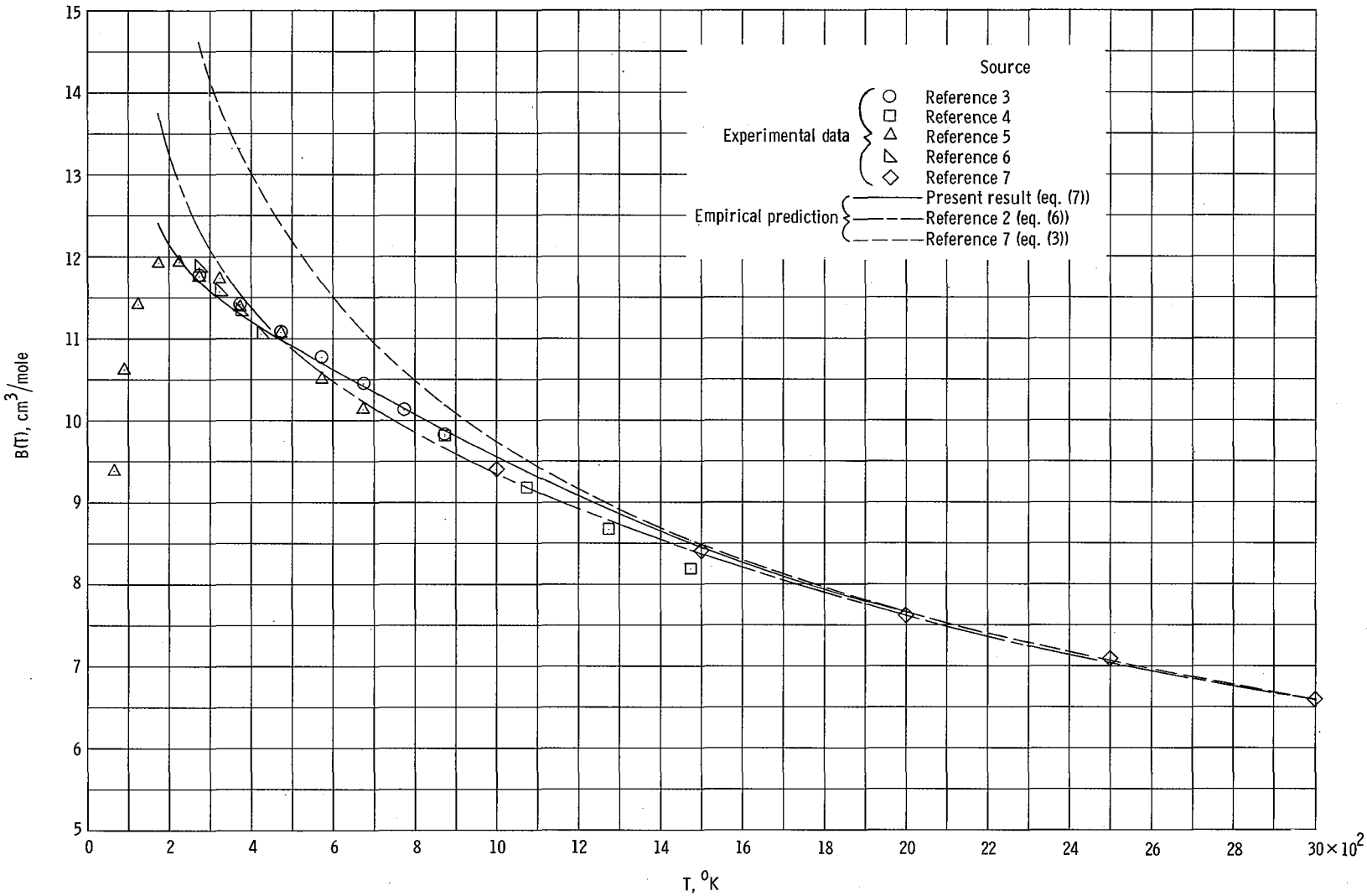

Figure 1.- Second virial coefficient for helium as a function of temperature.

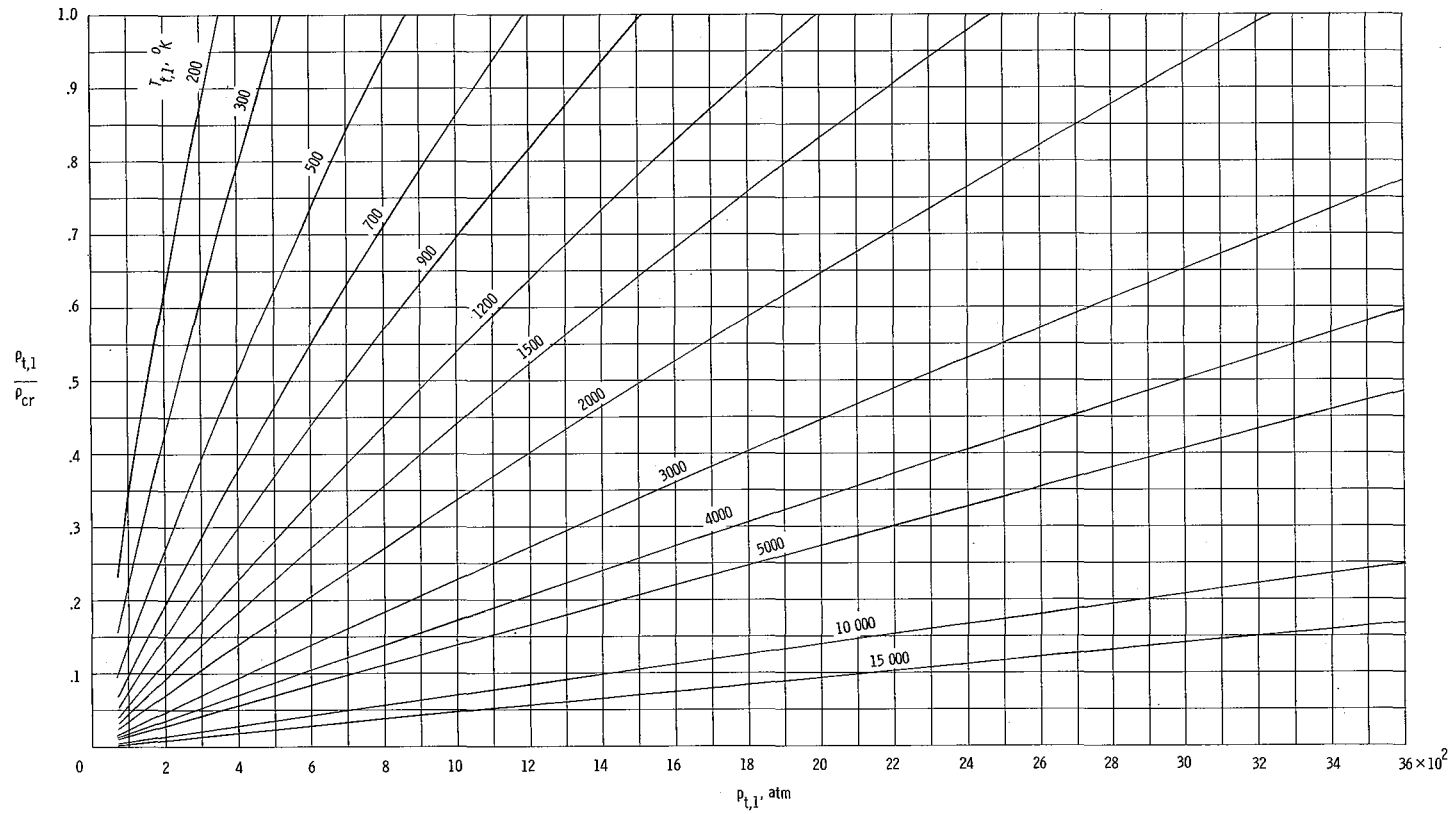

(a) $\rho_{t,1}/\rho_{cr}$; $\rho_{cr} = 1.7312 \times 10^{-2}$ mole/cm^3.

Figure 2.- Reservoir thermodynamic parameters for helium as a function of reservoir pressure for various reservoir temperatures.

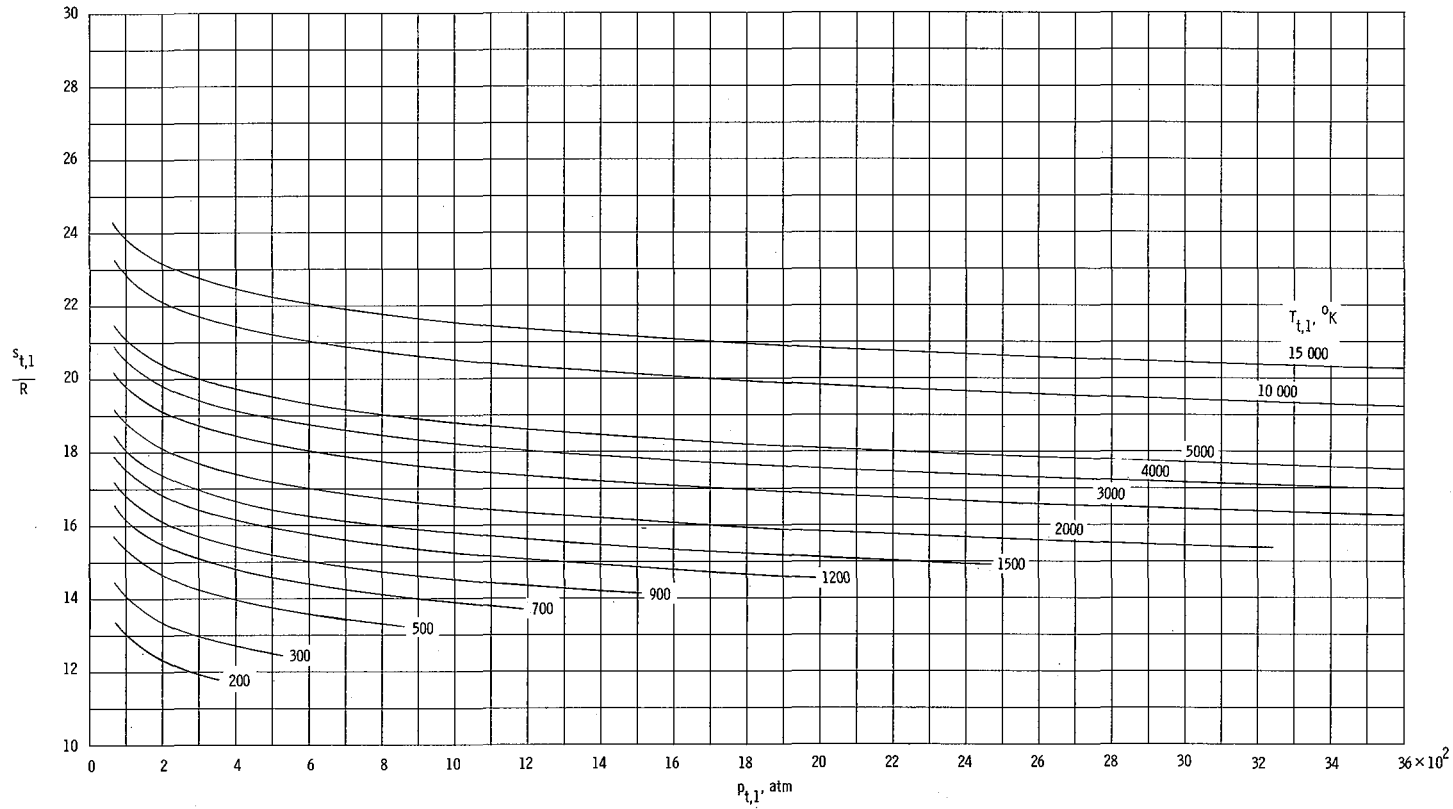

(b) $s_{t,1}/R$.

Figure 2.- Continued.

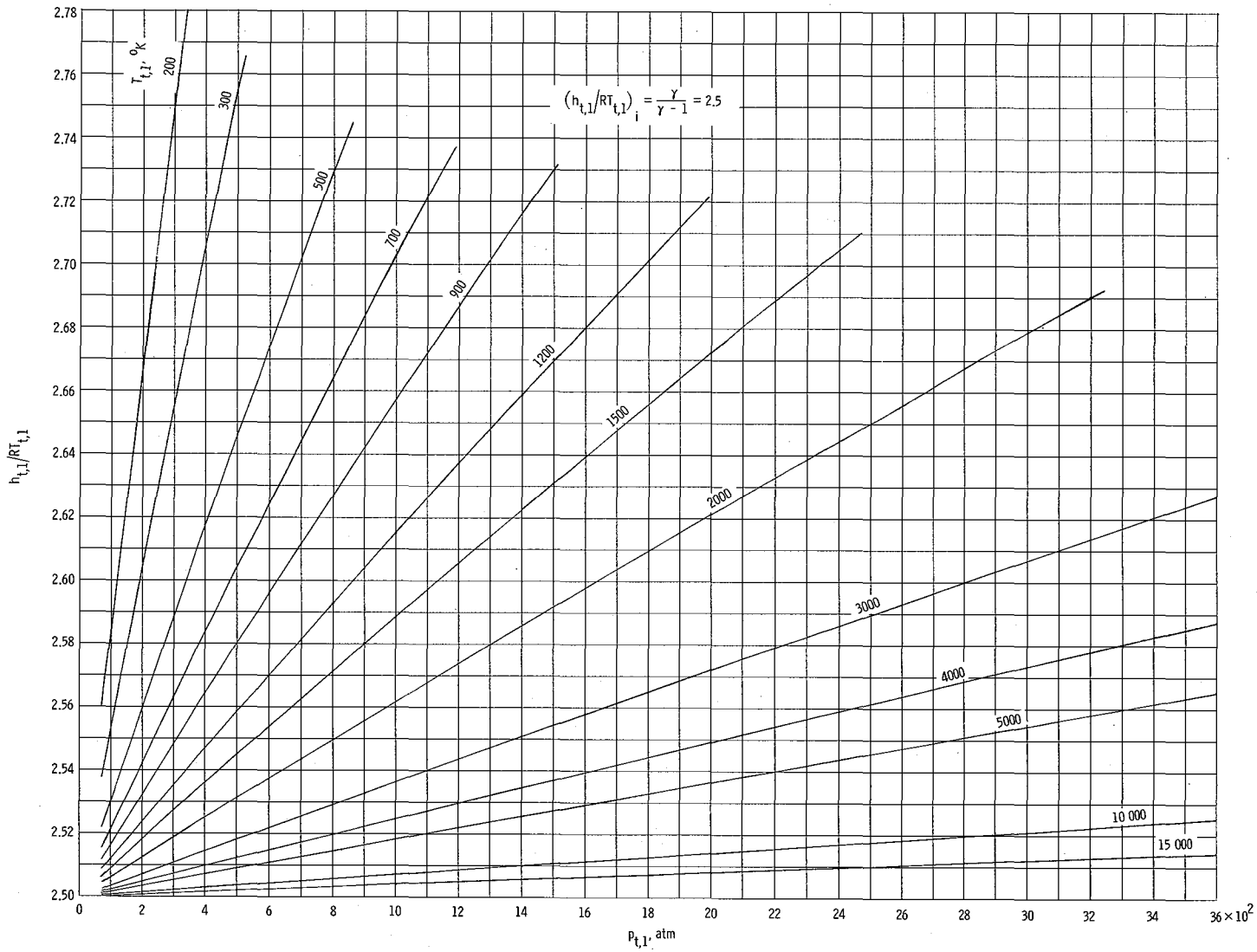

(c) $h_{t,1}/RT_{t,1}$.

Figure 2.- Continued.

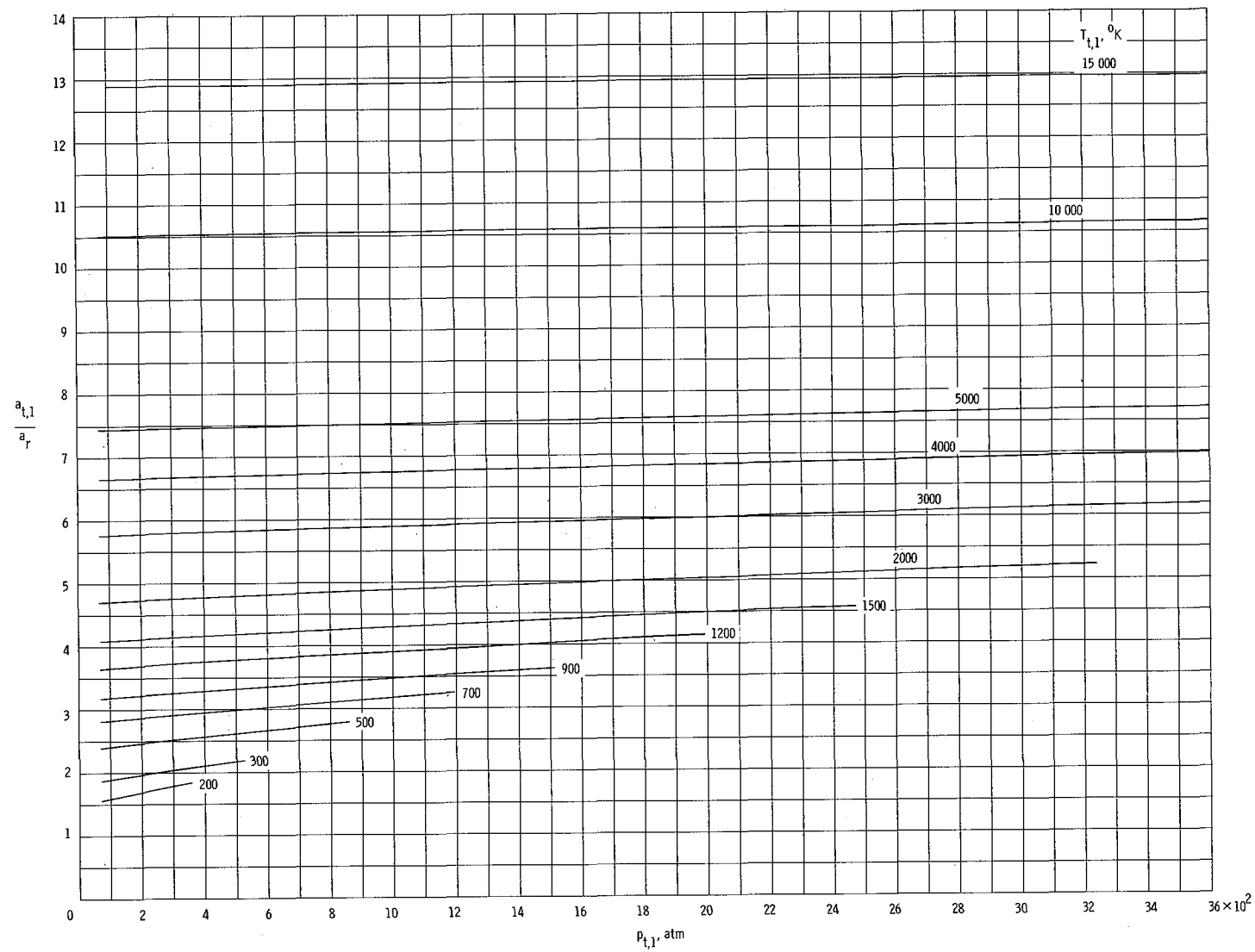

(d) $a_{t,1}/a_r$; $a_r = 5.5910 \times 10^4$ cm/sec (a_r was chosen arbitrarily and corresponds to 1 atm and 90.2° K (ref. 10).)

Figure 2.- Continued.

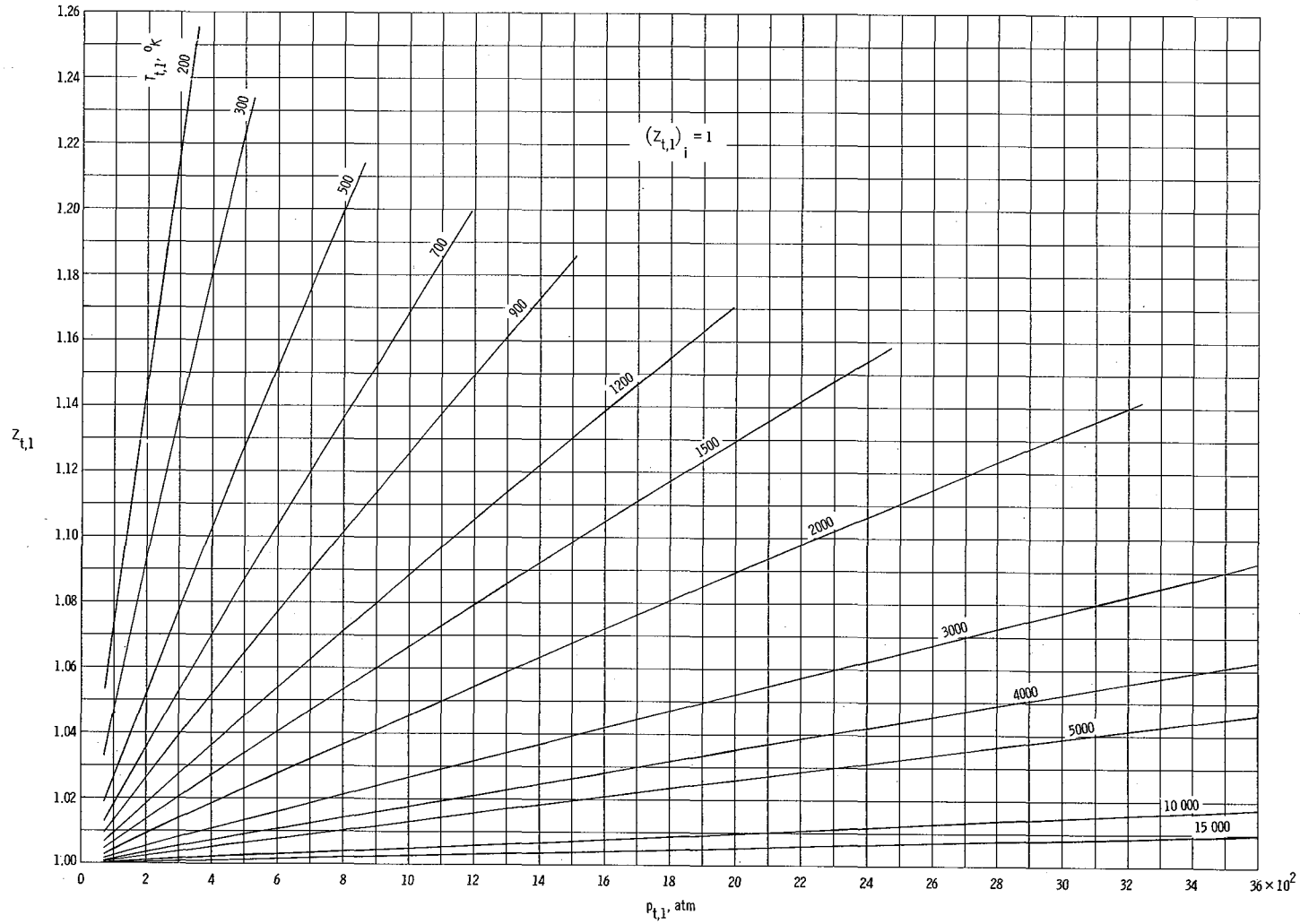

(e) $Z_{t,1}$.

Figure 2.- Concluded.

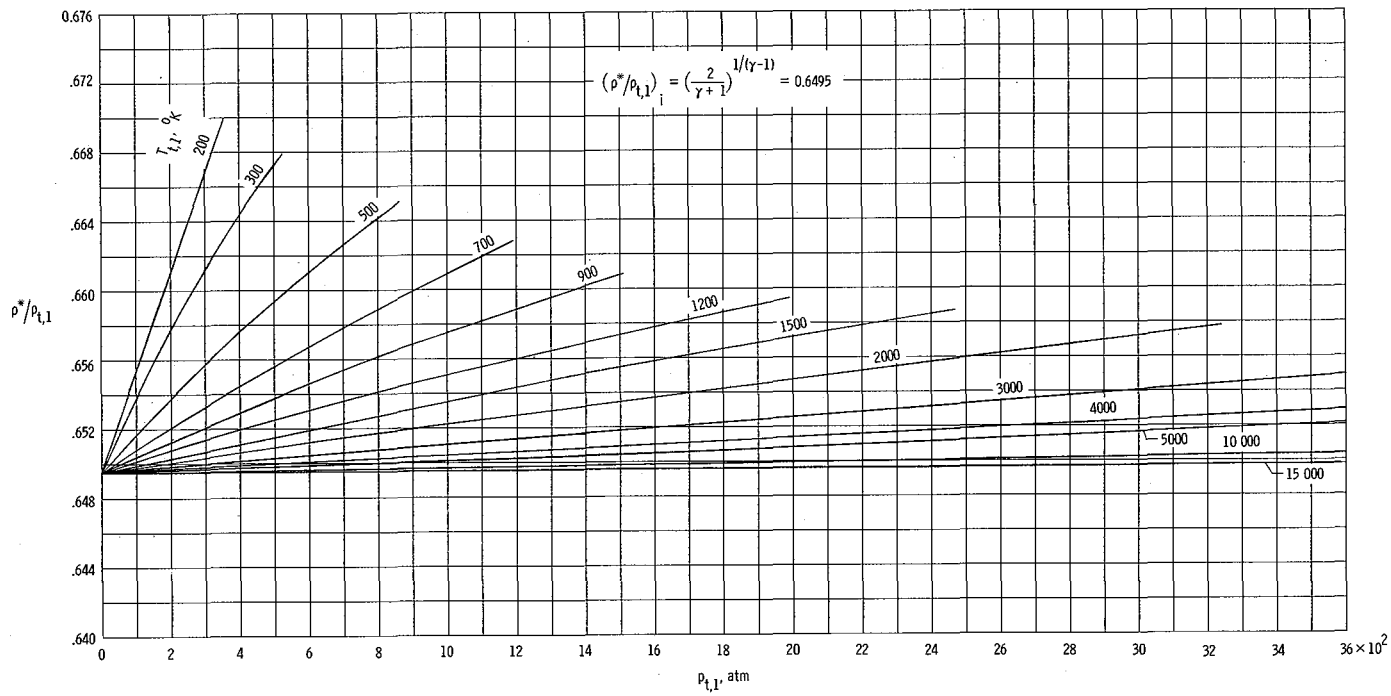

(a) $\rho^*/\rho_{t,1}$.

Figure 3.- Nozzle-throat parameters for helium as a function of reservoir pressure for various reservoir temperatures.

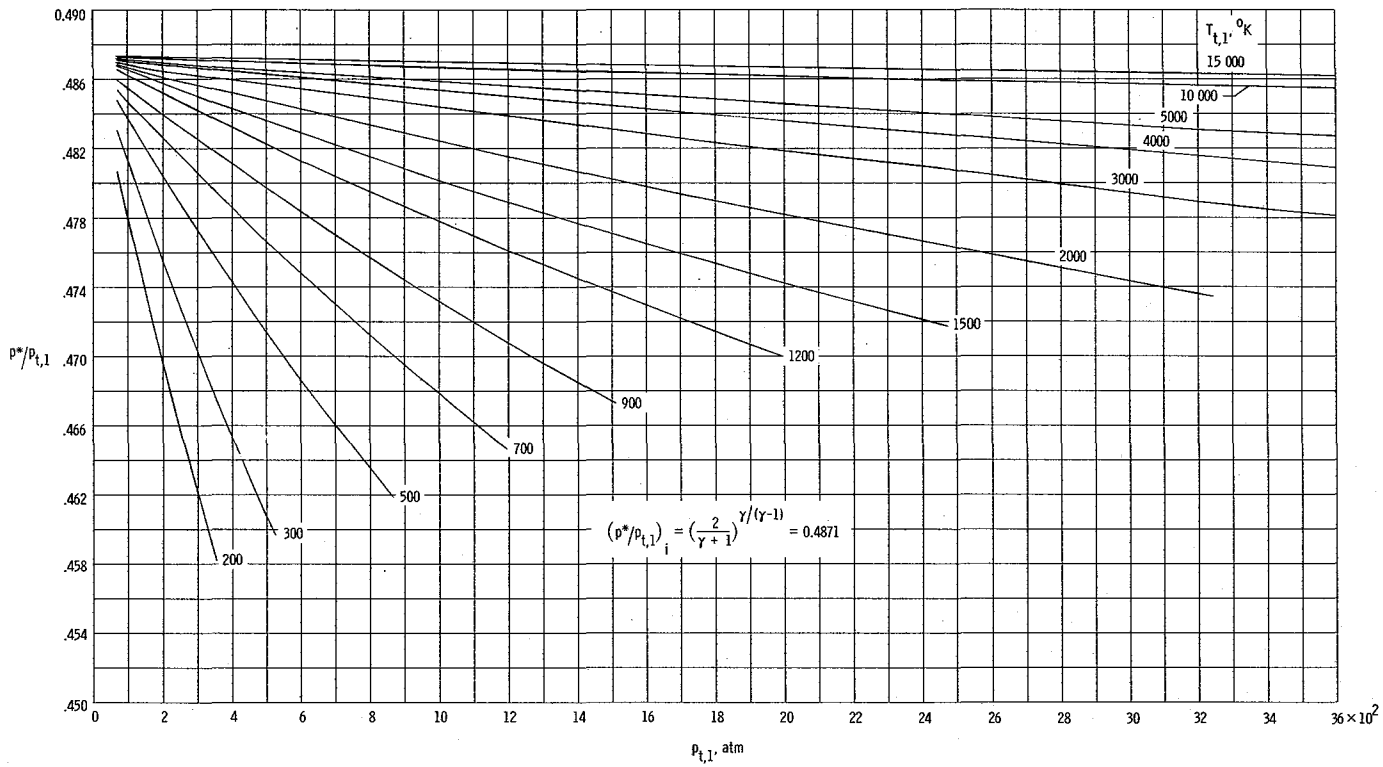

(b) $p^*/p_{t,1}$.

Figure 3.- Continued.

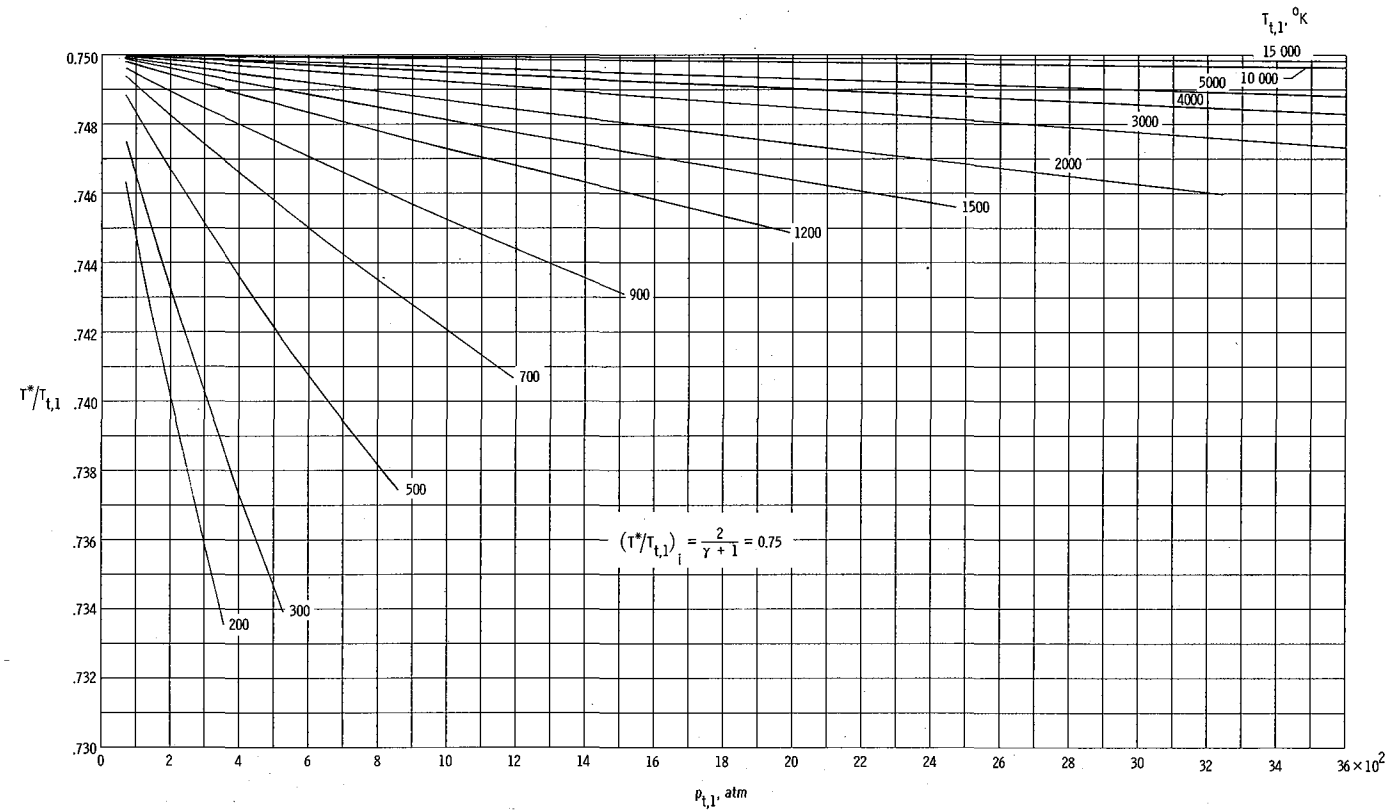

(c) $T^*/T_{t,1}$.

Figure 3.- Continued.

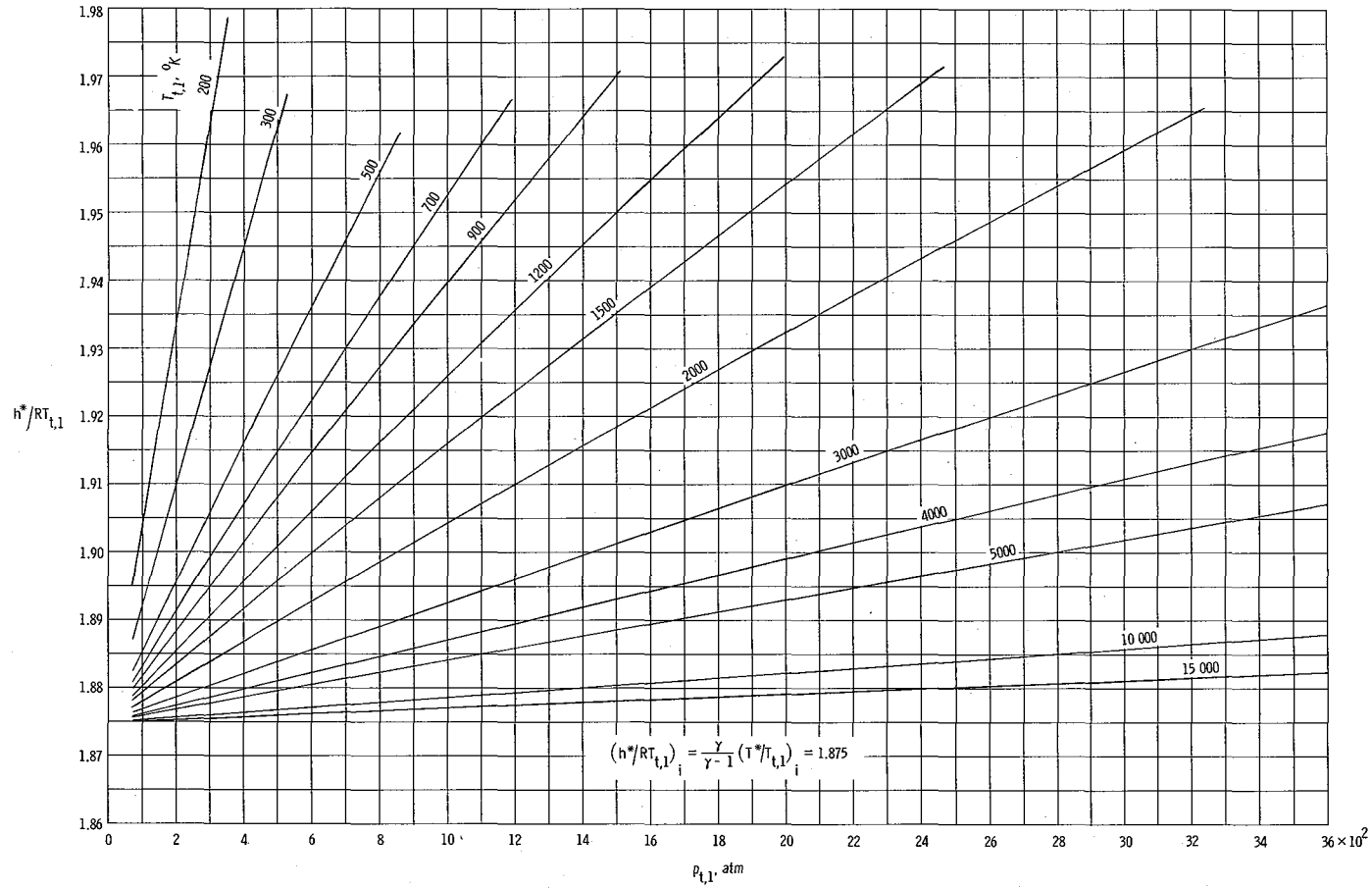

(d) $h^*/RT_{t,1}$.

Figure 3.- Continued.

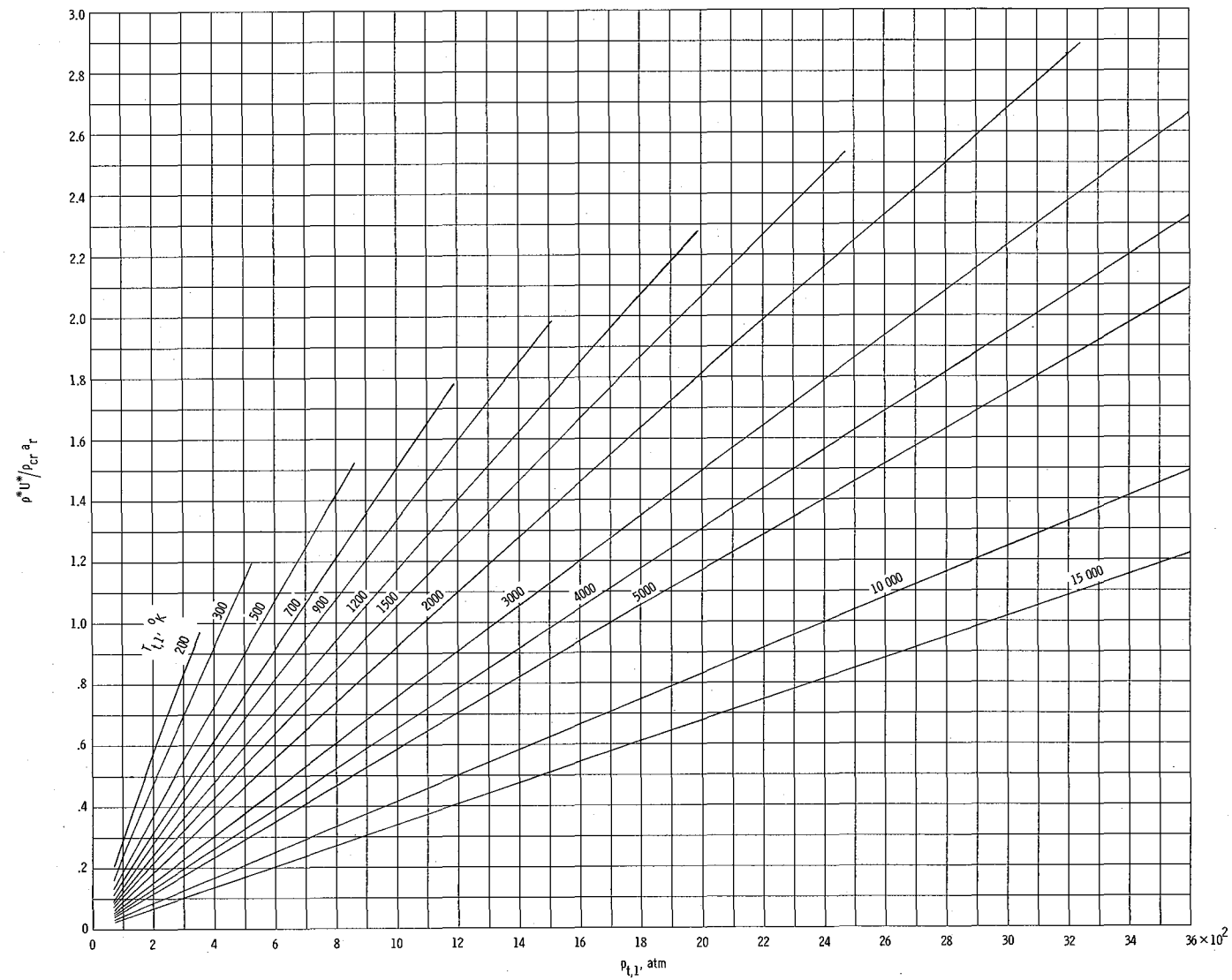

(e) $\rho^* U^*/\rho_{cr} a_r$; $\rho_{cr} a_r = 9.6791 \times 10^2$ moles/cm^2-sec.

Figure 3.- Concluded.

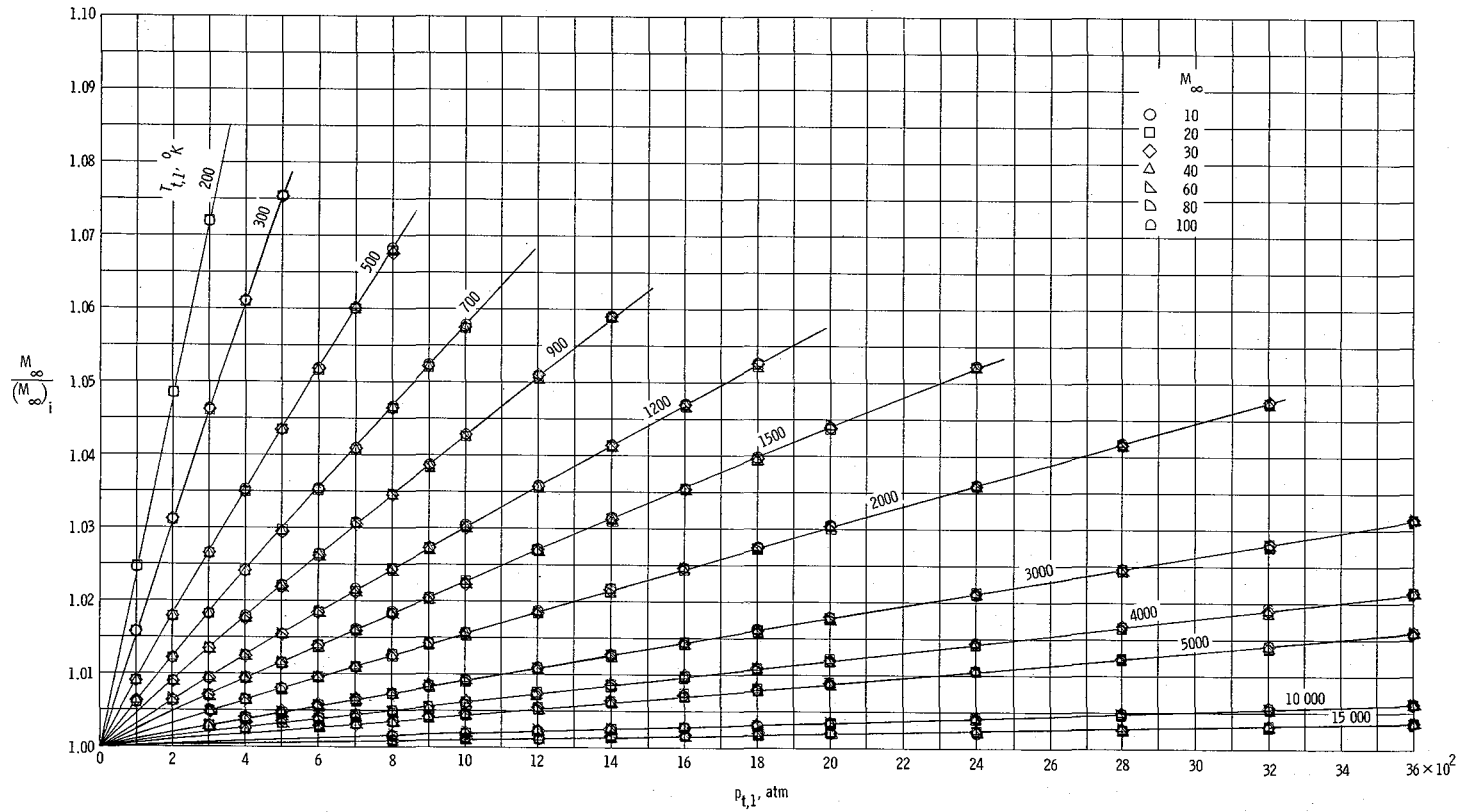

(a) M_∞.

Figure 4.- Ratio of real to ideal flow parameters for helium as a function of reservoir pressure for various reservoir temperatures and Mach numbers.

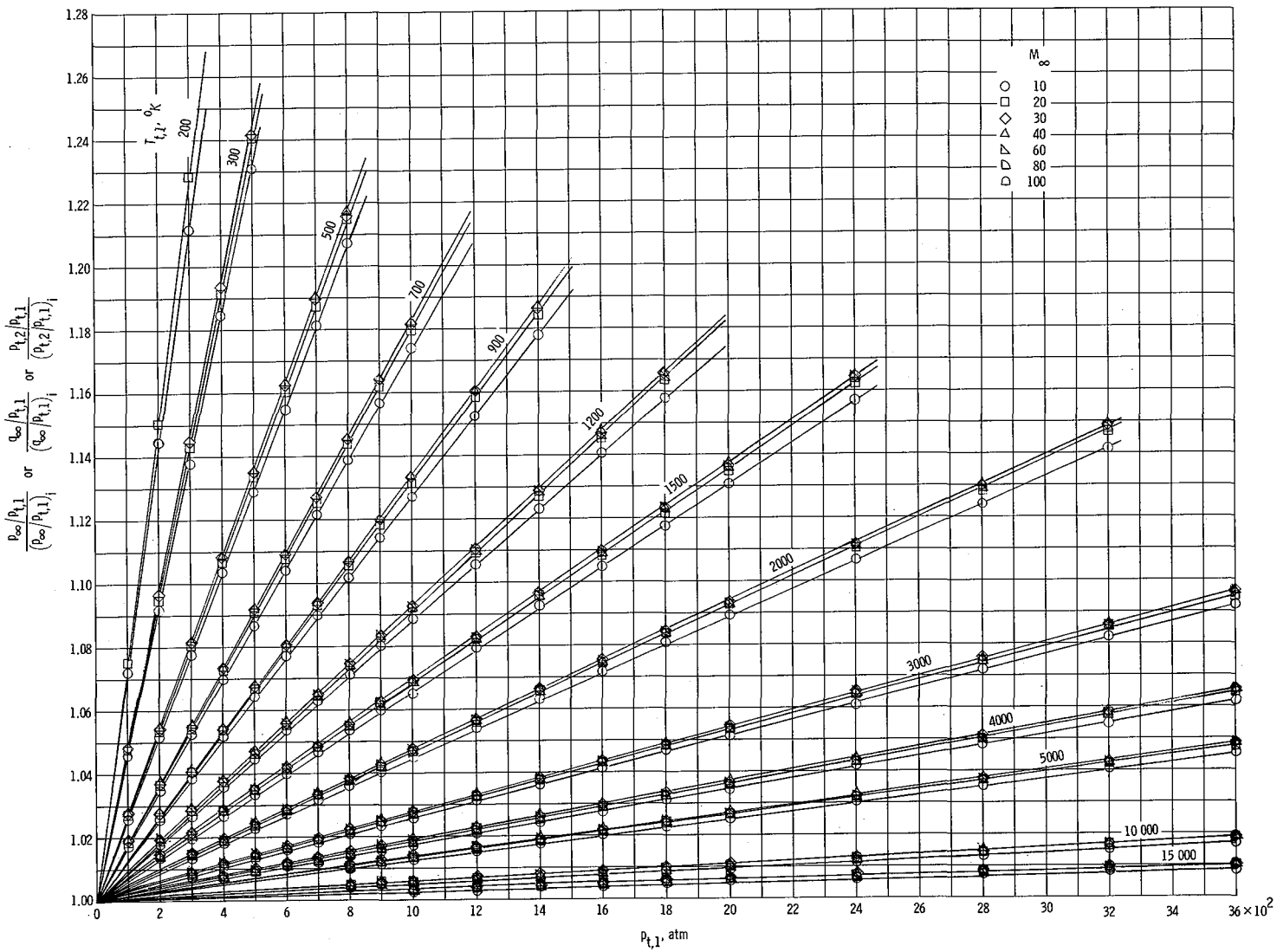

(b) $p_\infty/p_{t,1}$ or $q_\infty/p_{t,1}$ or $p_{t,2}/p_{t,1}$.

Figure 4.- Continued.

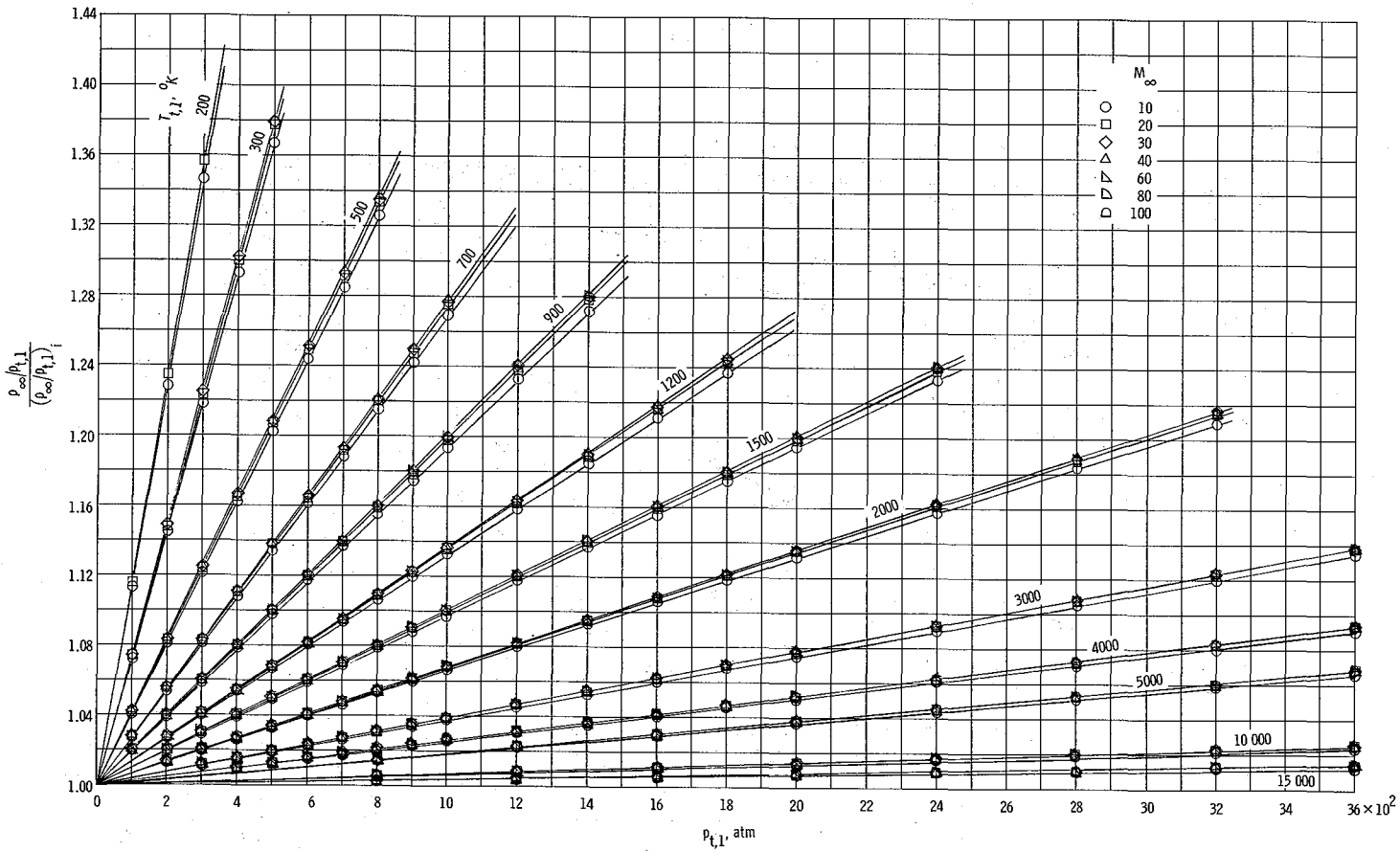

(c) $\rho_\infty/\rho_{t,1}$.

Figure 4.- Continued.

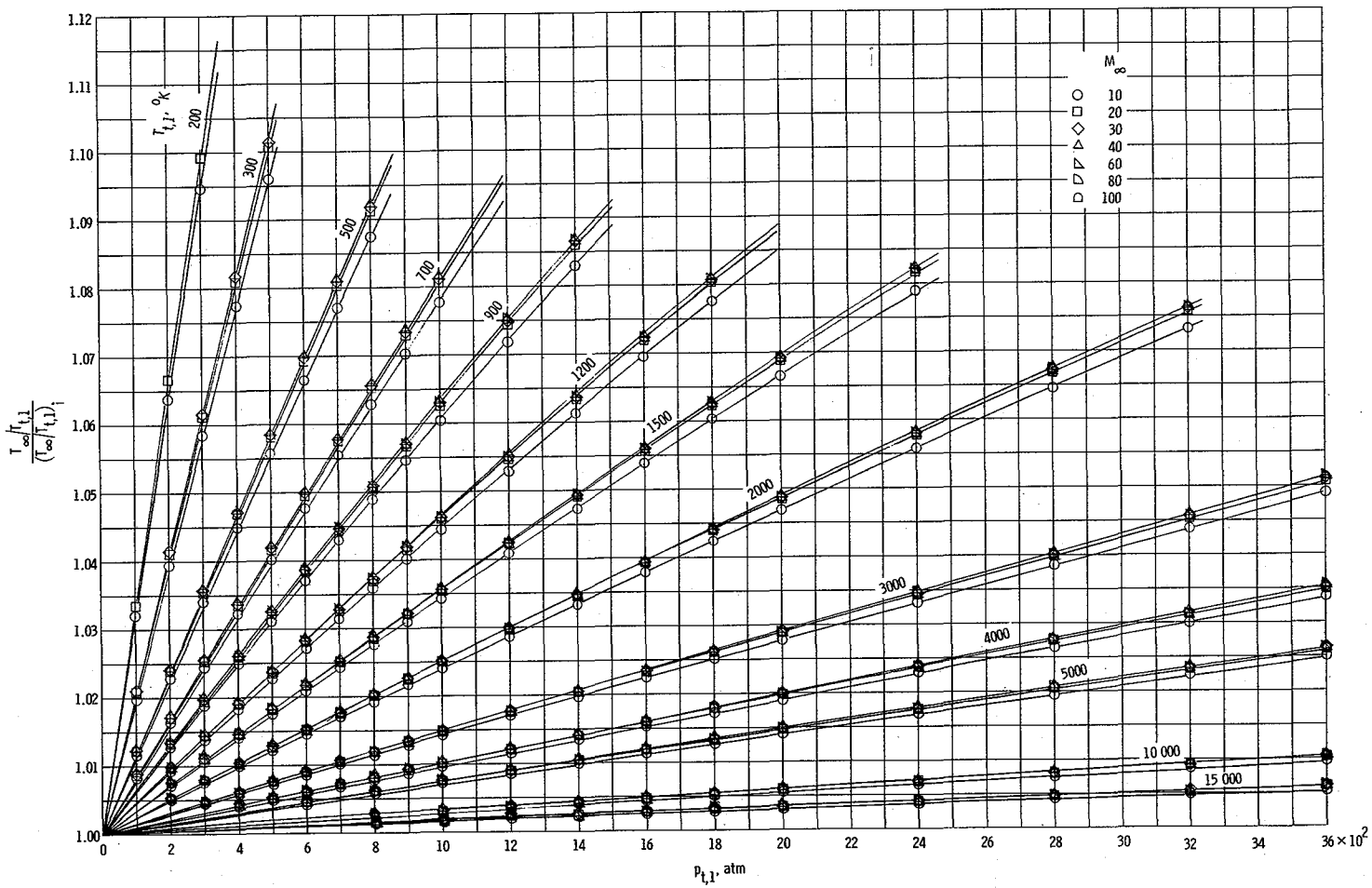

(d) $T_\infty/T_{t,1}$.

Figure 4.- Continued.

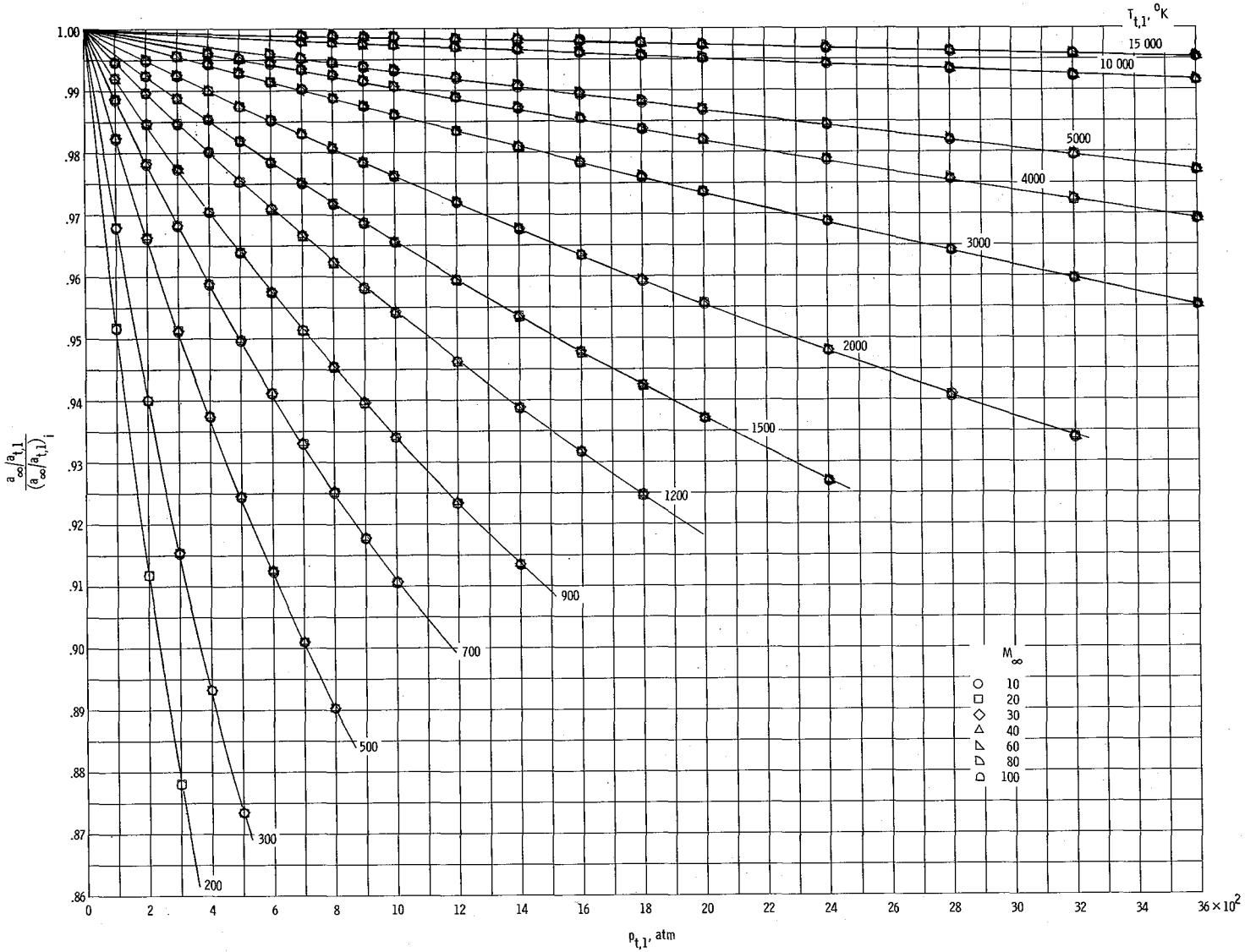

(e) $a_\infty/a_{t,1}$.

Figure 4.- Continued.

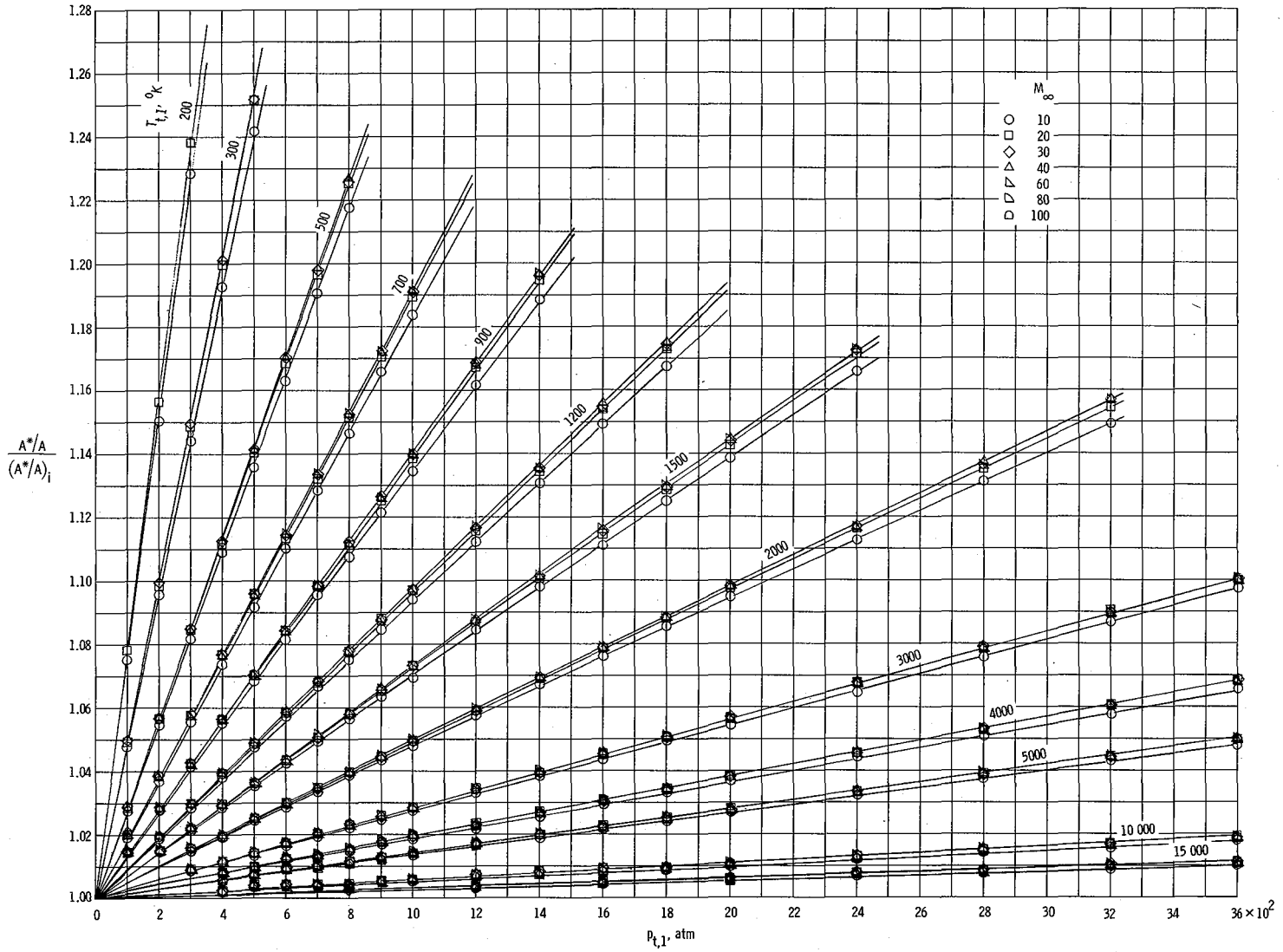

(f) A^*/A.

Figure 4.- Concluded.

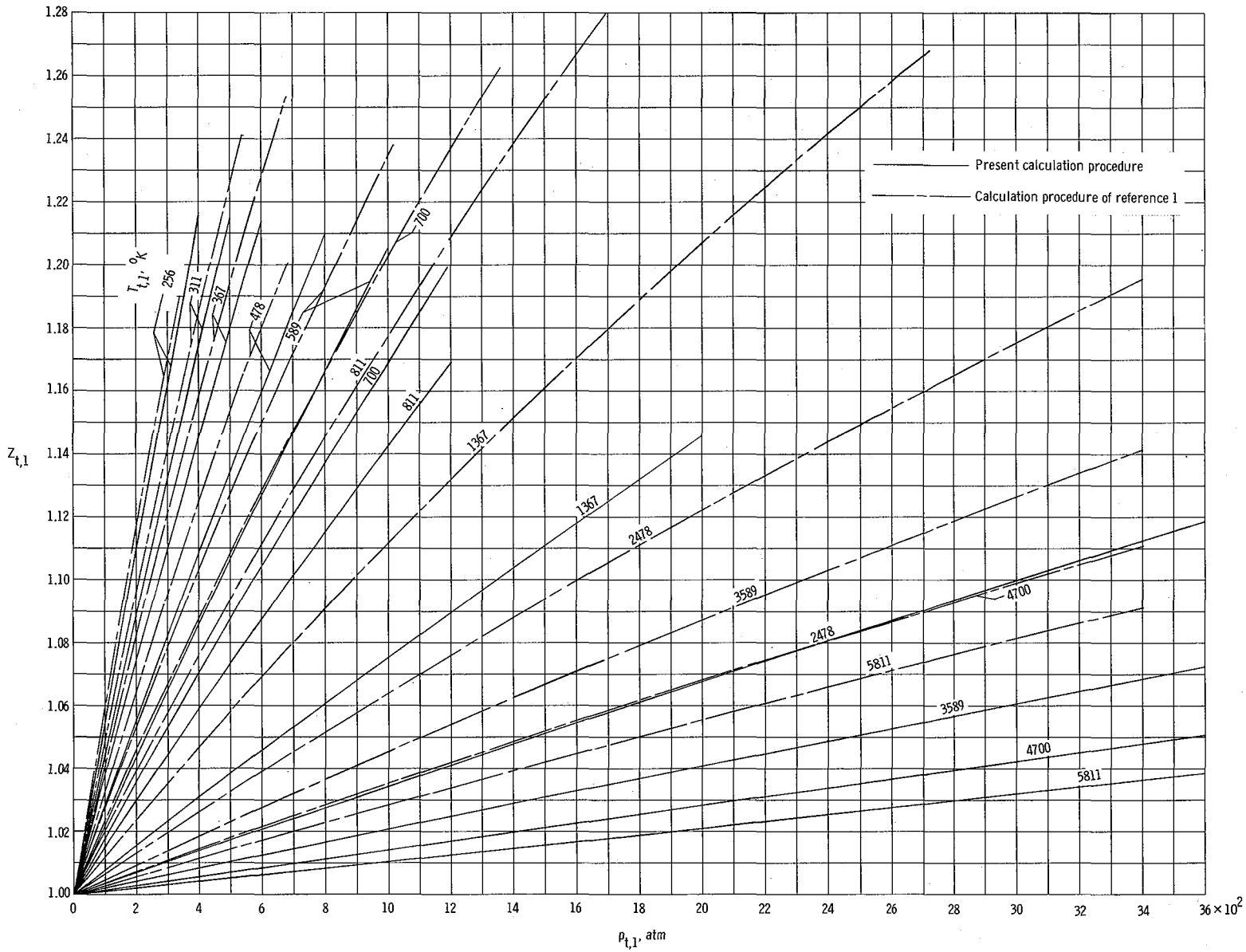

Figure 5.- Comparison of compressibility factors obtained with present calculation procedure and those of reference 1.

NATIONAL AERONAUTICS AND SPACE ADMINISTRATION
WASHINGTON, D. C. 20546

OFFICIAL BUSINESS

FIRST CLASS MAIL

POSTAGE AND FEES PAID
NATIONAL AERONAUTICS AND
SPACE ADMINISTRATION

POSTMASTER: If Undeliverable (Section 158
Postal Manual) Do Not Return

"The aeronautical and space activities of the United States shall be conducted so as to contribute . . . to the expansion of human knowledge of phenomena in the atmosphere and space. The Administration shall provide for the widest practicable and appropriate dissemination of information concerning its activities and the results thereof."

—NATIONAL AERONAUTICS AND SPACE ACT OF 1958

NASA SCIENTIFIC AND TECHNICAL PUBLICATIONS

TECHNICAL REPORTS: Scientific and technical information considered important, complete, and a lasting contribution to existing knowledge.

TECHNICAL NOTES: Information less broad in scope but nevertheless of importance as a contribution to existing knowledge.

TECHNICAL MEMORANDUMS: Information receiving limited distribution because of preliminary data, security classification, or other reasons.

CONTRACTOR REPORTS: Scientific and technical information generated under a NASA contract or grant and considered an important contribution to existing knowledge.

TECHNICAL TRANSLATIONS: Information published in a foreign language considered to merit NASA distribution in English.

SPECIAL PUBLICATIONS: Information derived from or of value to NASA activities. Publications include conference proceedings, monographs, data compilations, handbooks, sourcebooks, and special bibliographies.

TECHNOLOGY UTILIZATION PUBLICATIONS: Information on technology used by NASA that may be of particular interest in commercial and other non-aerospace applications. Publications include Tech Briefs, Technology Utilization Reports and Notes, and Technology Surveys.

Details on the availability of these publications may be obtained from:

SCIENTIFIC AND TECHNICAL INFORMATION DIVISION

NATIONAL AERONAUTICS AND SPACE ADMINISTRATION

Washington, D.C. 20546